



The future of extreme meteorological fire danger under climate change scenarios for Iberia

Virgilio A. Bento^{a,*}, Daniela C.A. Lima^a, Luana C. Santos^a, Miguel M. Lima^a, Ana Russo^a, Silvia A. Nunes^a, Carlos C. DaCamara^a, Ricardo M. Trigo^a, Pedro M.M. Soares^a

^a Universidade de Lisboa, Faculdade de Ciências, Instituto Dom Luiz, Lisboa, Portugal



ARTICLE INFO

Keywords:
 Fire weather index
 Atmospheric instability
 Iberian peninsula
 Euro-CORDEX
 Multi-model ensemble

ABSTRACT

Wildfires are disturbances that occur in ecosystems, both naturally and derived from anthropogenic factors, often caused by extreme meteorological conditions, and have recurrently destructive impacts on forests throughout the world. The complex nature of the interactions between wildfires, their dynamics, and human interference from a climate change perspective has motivated a growing number of researchers to address this topic. The fire weather index (FWI) has been extensively used to analyze the link between meteorological fire danger and its local to regional characteristics contributing to the severity of these events, as well as real-time operational monitoring at national and international levels. Recently, a new improved fire danger index that includes the effect of atmospheric instability has been developed, the so-called FWIe. The presence of instability in the atmosphere may be a boost to more energetic wildfires, such as the June 2017 extreme event in central Portugal, making it an important asset in risk monitoring and management. Here, a comprehensive examination of future fire risk on the Iberian Peninsula was performed. Additionally, a comparative analysis between FWI and FWIe was pursued in the context of climate change. We computed both FWI and FWIe using a multi-model ensemble composed of 13 Euro-CORDEX Regional Climate Model (RCM) simulations forced by different global climate models. The historical period (1971–2000) and three projected periods of 30 years (2011–2040, 2041–2070, and 2071–2100), under three emission scenarios (RCP2.6, RCP4.5, and RCP8.5) were considered. When assessing modelled FWI and FWIe, results show that summer values tend to substantially increase in the future when assuming the historical period as the benchmark, with an expected extension of the danger period to June and, in a lower magnitude, to September. The north-western region of Iberia, including the north of Portugal and the north-western-to-central Spain are the regions with larger increases in danger in the future, which may be critical since these are the regions with more fire-prone vegetation. This work also points to large differences in fire danger projections among scenarios, calling for a distinct set of adaptation needs that should be timely prepared by stakeholders and authorities.

1. Introduction

Wildfires are some of the most important disturbances to forests and its ecosystems all over the globe, with striking examples in Australia (Boer et al., 2020), California (Keeley and Syphard, 2021), or the Amazon Forest (Libonati et al., 2021). In Europe, the Mediterranean basin represents the most frequently fire-plagued region (Pausas and Fernández-Muñoz, 2012), with countries like Portugal (Trigo et al., 2006; Turco et al., 2019), Spain (Rodrigues et al., 2019), Italy (Salis et al., 2013), and Greece (Gouveia et al., 2016) being recurrently struck by these events. The destructive impacts of wildfires also affect

infrastructures, undermining the economy, and threatening human lives and health (Augusto et al., 2020; Molina-Terrén et al., 2019; Oliveira et al., 2020). One of the most tragic fire seasons of the last decades in south-western Europe was the extended summer season of 2017 in Portugal, where two large fire events, that took place in June and October, were responsible for about 300 thousand hectares of burnt area and more than 110 human fatalities (ICNF, 2017). Hence, the characterization and understanding of wildfires and its components has been a major scientific endeavor in the last decades.

One of the most well-known and widely used meteorological fire danger indices is the Canadian forest fire weather index system

* Corresponding author.

E-mail address: vabento@ciencias.ulisboa.pt (V.A. Bento).

(CFFWIS), which consists of six components that account for the effects of fuel moisture and weather conditions on fire behavior (van Wagner, 1974). The first three of the CFFWIS components consist of fuel moisture codes, representing numerical assessments of the moisture content in the forest floor and other dead organic matter. These ratings rise as moisture content decreases. A specific fuel moisture code corresponds to each of the three fuel layers: litter and other fine fuels, loosely compacted organic layers of moderate depth, and deep, densely compacted organic layers (Stocks et al., 1989), which are the fine fuel moisture code (FFMC), Duff moisture code (DMC), and drought code (DC), respectively. The remaining three components are the initial spread index (ISI), which is a combination between FFMC and wind speed, the build-up index (BUI), which is a combination between DMC and DC, and finally the fire weather index (FWI), which is a combination between ISI and BUI (van Wagner, 1987). The FWI offers information on how favorable the meteorological conditions are to build up and spread a wildfire, in case an ignition is triggered, and, when calibrated, FWI is particularly suitable to assess meteorological fire danger over Mediterranean Europe (DaCamara et al., 2014). Indeed, FWI is now operationally working within the scope of the emergency management services in the EU Copernicus programme – the Fire Danger Forecast module of the European Forest Fire Information System (EFFIS) (San-Miguel-Ayanz et al., 2012) –, and within the EUMETSAT Satellite Application Facility for Land Surface Analysis (LSA SAF) (Trigo et al., 2011) as part of the Fire Risk Map product. However, despite its versatility and widespread use, it has been stressed that the FWI does not incorporate any component that considers the local (or regional) atmospheric instability, a feature that could be relevant in some regions (Hoinka and de Castro, 2003). A recent work proposed a way forward to alleviate that shortcoming, improving the FWI by the incorporation of atmospheric instability (Pinto et al., 2020), through the inclusion of the Continuous Haines Index (CHI). This new enhanced index can be used to ameliorate estimates of the probability of exceedance of energy released by fires. To achieve this, a Generalized Pareto (GP) model was considered, and the authors showed that by using a steplike methodology that allows combining FWI and CHI as covariates of the GP parameters, an improved model is obtained that allows defining an enhanced FWI (hereafter denoted FWIe). For instance, Pinto et al. (2020) showed that FWIe may be a relevant source of information in cases of mild FWI associated with very high instability in the atmosphere (high CHI) where the danger is often underestimated, and in cases with very high FWI that can actually be associated to more moderate fire danger due to the presence of a very stable atmosphere (low CHI).

Climate change is expected to affect the frequency and intensity of wildfires in the future (Bowman et al., 2020; Dupuy et al., 2020; Jones et al., 2022; Turco et al., 2018), which heightens the vulnerability of regions located in Mediterranean climate types. An example is California, where climate change is increasing the likelihood of autumn days with extreme fire weather twofold (Goss et al., 2020). Another particularly vulnerable region is Iberia (Sousa et al., 2015), a prominent climate change hot spot (Alessandri et al., 2014; Diffenbaugh and Giorgi, 2012). With the aim of studying climate change impacts and consequences, at the local and regional scales, experiments to dynamically or statistically downscale global climate models (GCMs) were designed within projects such as the Coordinated Regional Downscaling Experiment (CORDEX) (Giorgi et al., 2009; Jacob et al., 2020). CORDEX effort aims to deliver frameworks for a coordinated model evaluation and climate projections, and an interface to the users of climate simulations concerning climate change impact, adaptation, and mitigation studies. EURO-CORDEX is the European branch of the CORDEX initiative which produced ensemble climate simulations based on multiple dynamical downscaling models forced by multiple GCMs from the Coupled Model Intercomparison Project Phase 5 (CMIP5). EURO-CORDEX simulations have been widely evaluated for present climate, revealing significant improvements in simulating the temporal and spatial variability of the European climate (Katrakou et al., 2015;

Kotlarski et al., 2014; Prein et al., 2016; Vautard et al., 2013). Recently, Herrera et al. (2020) assessed the skill of EURO-CORDEX RCMs in representing the precipitation and temperature over the Iberian Peninsula, showing a good spatial agreement among simulations and observations. A similar assessment was performed by Soares et al. (2017a) and Cardoso et al. (2019) over Portugal, revealing a good agreement between the multi-model EURO-CORDEX ensemble and observations, with substantial gains when compared to previous regional climate projects like PRUDENCE and ENSEMBLES (Soares et al., 2012). The added value of using high-resolution EURO-CORDEX simulations was quantified by Soares and Cardoso (2018), revealing significant added value in the representation of precipitation patterns over Europe, particularly for extremes. More recently, the same method was applied for temperature (Cardoso and Soares 2022) and wind (Molina et al., 2023) over Europe, for precipitation and temperature over the Iberian Peninsula (Careto et al., 2022a, 2022b), and for temperature over the Alps (Soares et al., 2022). Other studies also revealed the added value of using RCMs to assess climate means and extremes (e.g., Rummukainen, 2016; Casanueva et al., 2016). EURO-CORDEX RCMs were also able to represent the near-surface wind speed onshore (Moemken et al., 2018; Nogueira et al., 2019; Vautard et al., 2013) and offshore (Soares et al., 2017b). Based on a large ensemble of continental-scale simulations from EURO-CORDEX, several works focused on the assessment of changes induced by global warming on key wildfire-related meteorological variables, such as precipitation (Jacob et al., 2014; Prein et al., 2016; Soares et al., 2017a), temperature (Cardoso et al., 2019a; Jacob et al., 2014; Vautard et al., 2013), and wind (Nogueira et al., 2019; Soares et al., 2017b) in the Iberian Peninsula. These studies have steadily projected a decrease in mean precipitation, together with an increase in extreme precipitation events (Soares et al., 2017a); a significant increase in maximum and minimum temperatures spanning all seasons and emission scenarios (Cardoso et al., 2019); and a reduction in 10-m wind speed over northern Portugal during winter and autumn (Nogueira et al., 2019), whilst a small increase during summer over central Portugal. Furthermore, several works have taken advantage of the CORDEX multi-model approach to directly analyze future projections of wildfire danger in different regions (Faggian, 2018; Fargeon et al., 2020; Ruffault et al., 2018; Trnka et al., 2021; Varela et al., 2019). A recent work (Calheiros et al., 2021) focusing on the Iberian Peninsula, used EURO-CORDEX models to assess the impact of climate change on the spatial distribution of pyro-regions by taking advantage of CFFWIS components. However, Calheiros et al. (2021) only looked at RCP4.5 and RCP8.5, lacking the heavily mitigated RCP2.6, which is also relevant in terms of adaptation measures.

The Iberian Peninsula fire regime is particularly susceptible to weather and climate variability, where extreme events such as heatwaves and droughts, and anomalous atmospheric circulation patterns are typically associated with high incidence of fires (Parente et al., 2018; Pereira et al., 2005; Russo et al., 2017). Wildfires in the region are characterized by a main summer fire season and by a secondary spring peak that is more evident over the northern regions (Trigo et al., 2016). The Iberian Peninsula presents itself as a key region of study in terms of wildland fire adaptation and mitigation plans for the next decades. Indeed, active forest and fire management practices are seen as a tool to mitigate the impacts of climate change in these events. Nevertheless, such management decisions from authorities and decision makers must be timely informed to be effective. With this study we intend to present a comprehensive analysis of the impact of climate change on fire danger in Iberia, using a EURO-CORDEX weighted multi-variable multi-model ensemble to estimate both FWI and FWIe. The use of weighted multi-model ensembles in climate studies has been shown to improve climate projections derived from ensembles (Brunner et al., 2019; Christensen et al., 2010; Eyring et al., 2019; Knutti et al., 2017; Lorenz et al., 2018; Nogueira et al., 2019; Sanderson et al., 2017; Soares et al., 2012; Wenzel et al., 2016), allowing to generate more reliable regional climate projections and constrain the uncertainty of climate modelling.

This study expands the framework for using FWI with projections of atmospheric instability into the future, addressing a critical component of wildfires that has received limited attention in previous research. For instance, Dowdy et al. (2019) used the McArthur Forest Fire Danger Index (FFDI), instead of FWI, to represent near-surface weather conditions and the Continuous Haines Index (CHI) to characterize lower to mid-tropospheric vertical stability. In addition, this investigation considers a weighted multi-model ensemble based on a multi-variable quality analysis that encompasses the three Representative Concentration Pathways (RCP) emission scenarios. The study's key objective is to strengthen the understanding on how fire danger in the Iberian Peninsula is projected to change in the future by taking advantage of a state-of-the-art index such as the enhanced FWIe and considering the three RCPs. To accomplish that, two specific objectives were pursued:

- Computing FWI and FWIe using the output of a set of EURO-CORDEX RCM simulations downscaled from different GCMs for the historical and for three future periods under three emission scenarios: RCP2.6, RCP4.5, and RCP8.5.
- Estimating the number of days in each period with FWI larger than the 90th percentile. The anomaly in the number of days obtained in the future and historical periods is estimated for a weighted multi-model ensemble of FWI and FWIe, and the differences between the two are analysed.

This analysis provides a clear insight on how atmospheric instability may change the evolution of fire danger extremes when comparing with the original surface-based fire weather index. Finally, we aim at producing the needed fire danger information to assist decision-makers on the different adaptation needs associated with the diverse mitigation targets.

2. Data and methods

2.1. EURO-CORDEX model data

The current study is focused on the Iberian Peninsula, and the regionalization described in Trigo et al. (2016) is adapted here. The authors used the burned area associated to 66 autonomous regions (AR) in Portugal and Spain and normalized it by each AR area to obtain the normalized burned area. Then, a cluster analysis, using the K-means algorithm, was applied to the NBA of the 66 ARs, and finally retained four statistically significant clusters (Fig. 1). These include a north-western cluster aggregating the northern half of Portugal and the extreme northwest of Spain (NW), a south-western cluster including the southern and interior regions of Portugal and central and south-western Spain (SW), an eastern cluster including the coast and pre-coastal areas east of Gibraltar until the Pyrenees (E), and a northern cluster corresponding to regions over the mountainous sectors of northern Spain, such as the Asturias, Calabria, and Basque Country (N).

The EURO-CORDEX high-resolution simulations were performed

under the CORDEX effort (Jacob et al., 2014, 2020) and provide a larger number of regional climate runs over a common domain. The runs here considered were produced with a grid of 0.11° horizontal resolution, dynamically downscaling the original CMIP5 GCM ensemble. Current climate simulations of EURO-CORDEX are run from 2006 onwards following different future scenarios of anthropogenic forcings: RCP2.6, RCP4.5, and RCP8.5. In this study, three projected periods were used and are referred as "future periods" onwards (namely, the begin-century 2011–2040, the mid-century 2041–2070, and the end-century 2071–2100). On the other hand, the historical period for these regional climate models is simulated from 1950 until 2005 following historical emissions. Hence, for this study the period 1971–2000 is selected as the historical period. It is worth noticing that the simulations are not synchronized in time due to GCMs forcing. These RCPs are defined according to the correspondent effect of greenhouse gas emissions in the radiative forcing values in 2100, which are +2.6, +4.5 and +8.5 Wm⁻² relative to pre-industrial era. Hence, the most mitigated scenario is the RCP2.6 and the less mitigated one is the RCP8.5. While in the former, the peak of global annual greenhouse gas emissions occurs between 2010 and 2020, for the latter the emissions grow continuously throughout the 21st century. Finally, the emissions of RCP4.5 peak around 2040 and lessen afterwards (Moss et al., 2010; Riahi et al., 2011; van Vuuren et al., 2011).

From the full set of EURO-CORDEX RCM simulations available in the Earth System Grid Federation (ESGF) data portal, we selected 13 sets (historical/future) of them as these were the only ones that were run for the historical and future scenarios and the 3 RCP emission scenarios (Table 1). Both fire danger indices FWI and FWIe are computed for the 13-model ensemble.

In this study, a new multi-variable approach to build a multi-model ensemble is used to assess future meteorological fire danger conditions, using two fire weather indices (FWI and FWIe). Since both indices need

Table 1

EURO-CORDEX RCMs used in this study, along with the responsible institute and the forcing GCMs. The 13 simulations have historical, RCP2.6, RCP4.5, and RCP8.5 scenarios.

RCM	Institute	GCM	Reference
CCLM4-8-17	CLM	EC-Earth	Rockel et al. (2008)
ALADIN63	CNRM	CNRM-CM5	Colin et al. (2010)
HIRHAM5	DMI	EC-Earth	Christensen et al. (2007)
		HadGem2-ES	
REMO2015	GERICS	NorESM1-M	Jacob et al. (2012)
RACMO22E	KNMI	CNRM-CM5	van Meijgaard et al., 2008
		EC-Earth	
		HadGem2-ES	
REMO2009	MPI	MPI-ESM-LR	Jacob (2001)
RCA4	SMHI	EC-Earth	Strandberg et al. (2014)
		HadGem2-ES	
		MPI-ESM-LR	
		NorESM1-M	

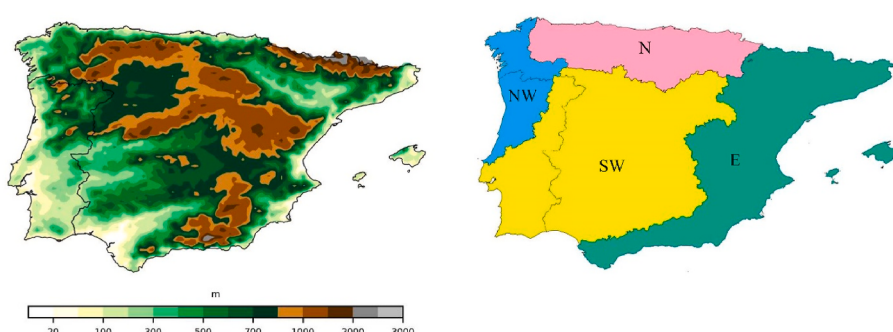


Fig. 1. Study region maps of (left) altitude and (right) the 4 pyro-regions following Trigo et al., (2016).

multi-variable information, this new approach is key to preserve the physical consistency among climate projections. An assessment of the performance of the 13 EURO-CORDEX RCMs in simulating precipitation, maximum and minimum temperatures was performed against the Iberia01 (IB-01) observational gridded dataset (Herrera et al., 2020) across the Iberian Peninsula. This procedure followed the methodology described in Lima et al. (2023a). The evaluation encompassed the historical period spanning from 1971 to 2000, employing a diverse range of error metrics, encompassing systematic and absolute errors, as well as properties related to distributions and extremes. These metrics included mean bias, mean absolute error, root mean squared error, normalized standard deviation, spatial correlation, Willmott-D Score, Perkins skill score, and Yule-Kendall skewness. Based on this evaluation, weights were derived for each model and variable, considering the individual model's performance in reproducing the observed climate (a comprehensive explanation of the methodology for computing model weights can be found in Lima et al. (2023a)). To incorporate the multi-variable performance, a distinct weight for each model was computed, where the contribution of precipitation weight amounted to 50%, while both maximum and minimum temperatures contributed equally, each accounting for 25% in the calculation of the final weight for each model. Subsequently, the multi-model ensemble was calculated employing these weights. In general, the weighted multi-model ensemble demonstrated good ability in representing both the averages and extremes of precipitation, as well as maximum and minimum temperatures when compared to IB-01 under current climatic conditions over Portugal (comparable outcomes were observed across the Iberian Peninsula; Lima et al., 2023a). This strengthens our confidence in its utilization for characterizing future climate extremes. Additionally, this innovative multi-variable approach augments the consistency in assessing fire danger conditions based on FWI and FWIe, since both indices are based on multi-variable information.

The list of daily meteorological variables needed for the development of this study include maximum and minimum 2-m temperature, surface pressure, specific humidity, daily accumulated precipitation, 10-m wind speed, 850 hPa and 500 hPa temperature, and 850 hPa specific humidity. Relative humidity is obtained from specific humidity, 2-m mean temperature is the simple average between maximum and minimum temperatures, the 700 hPa temperature was estimated by interpolating between 850 hPa and 500 hPa temperatures, and dew-point temperature at 850 hPa was computed from 850 hPa specific humidity.

2.2. Fire weather indices

The CFFWIS components were estimated following the procedure described by Van Wagner (1987), namely the Drought Code (DC), Duff Moisture Code (DMC), Fine Fuel Moisture Code (FFMC), Initial Spread Index (ISI), Build-up Index (BUI), and the Fire Weather Index (FWI). The first three have a memory component and are denominated the fuel moisture codes, based on consecutive daily observations of 2-m temperature, relative humidity, 10-m wind speed, and 24-h accumulated precipitation. The remaining three are the fire behaviour indices. Originally the indices are to be calculated at noon, however EURO-CORDEX only provides daily values of the variables needed. Hence, following other studies (Carvalho et al., 2009; Giannakopoulos et al., 2009; Moriondo et al., 2006), we computed the CFFWIS components based on daily mean 2-m temperature, relative humidity, and 10-m wind speed, and daily accumulated precipitation. Thus, FWI values (and therefore the other CFFWIS indices) are estimated on a daily basis for each grid-point of each individual model for the historical and future periods (over three different emission pathways).

We also computed FWIe (Pinto et al., 2020) that incorporates the Continuous Haines Index (CHI), which was designed to evaluate atmospheric instability (Haines, 1988) that promotes convective fires (Mills and McCaw, 2010). CHI is defined by an instability term (CA) based in the difference between temperature at 850 (T850) and 700 hPa (T700),

and by a moisture term (CB) based on the difference between temperature (T850) and dew point (DP850) at the lower level (850 hPa). The CHI is estimated for each grid cell of each model for the historical and future periods. Then, the FWIe is estimated as a function of FWI and CHI, calibrated so that the probability of exceedance of a pre-defined threshold of released energy on a Generalized Pareto dependent on FWI is identical to the one given by the more complex Generalized Pareto model dependent on both FWI and CHI. A comprehensive explanation and validation of the FWIe methodology can be found in Pinto et al. (2020).

A validation of FWI estimated with EURO-CORDEX regional models against FWI estimated with the fifth generation of the ECMWF atmospheric reanalysis ERA5 (Hersbach et al., 2019) is firstly undertaken. The reanalysis is used instead of observations due to the lack of some of the observed variables needed to compute FWI and FWIe in the region. ERA5 FWI and FWIe are computed using the same methodology described above for the EURO-CORDEX RCMs. The models' ability to reproduce the observed probability distribution functions (PDFs) was quantified by the Perkins skill score (S) (Perkins et al., 2007):

$$S = 100 \times \sum_{i=1}^B \min [E_{p,i}, E_{o,i}] \quad \text{Eq. 1}$$

where E_p and E_o are the simulated and observed empirical PDFs, respectively, $\min [E_{p,i}, E_{o,i}]$ is the minimum value between them, and B is the total number of bins. This score provides a measure of similarity between the simulated and observed empirical PDFs, with $S = 100\%$ if the model perfectly reproduces the observed empirical PDFs. Two different methods were used to estimate the S score, as described in Boberg et al. (2009). The first for the full PDF (the so-called S score), and the second for the average between two sections, where the first section comprises the data until the 90th percentile and the second from the 90th percentile onwards (the so-called S90 score).

2.3. Number of extreme FWI and FWIe days

Changes in the number of days with high fire danger in the future were computed as those exceeding the 90th percentile of fire danger. Percentiles were computed for each grid cell on a daily basis during JJAS. We focus on JJAS because atmospheric instability is stronger in summer months in the region of study (Pinto et al., 2020; Santos et al., 2023), and intense fire episodes tend to occur during this period.

During the historical period, which serves as our baseline, on average, there were about 12 days with high fire danger (i.e., exceeding the 90th percentile for each grid cell) for a total of 122 days in the 4-month summer (JJAS) considered. Anomalies in the number of days with high fire danger were then computed as the difference between the 30-year mean of days with high fire danger in the future, and the corresponding means in the historical period.

The accuracy of our percentile calculations is assured by following the procedure of Zhang et al. (2005) that avoids introducing artificial discontinuities in the percentile time-series that could arise at the beginning and end of the base period. It is worth noting that we compute the historical percentile for both FWI and FWIe on a daily basis, employing then a 5-day moving window filter to smooth. Such percentile-based approach mitigates the influence of biases in our results since it tailors each threshold to the specific characteristics of each grid point and model.

3. Results

FWI distributions from the multi-model ensemble are first compared with those from ERA5 (Figure S1). Results show S scores between modelled and observed PDFs typically above 70 %, and S90 scores above 80 %, which guarantees that the multi-model ensemble is able not only to reproduce the distribution of observed FWI, but also the tail of the

PDF, a critical feature to achieve the objectives of the present work.

Fig. 2 shows the ensemble mean monthly averaged historical (1971–2000) 90th percentile of FWI, FWIe, and the difference between the two. These maps help understanding the behavior of the variables in the extended summer period. As expected, values of fire weather indices increase from June to August and decrease in September. Absolute values of FWI and FWIe vary depending on the latitude, with values of the 90th percentile surpassing 50 in several southern regions in July and August and varying between 5 and 20 in most northern regions (supplementary material, **Figure S2**). The difference between FWI and FWIe shows a dichotomous behavior in Iberia. These differences are more evident in July and August, with larger FWIe in the southern halve of the peninsula, and larger FWI mostly located in the northern regions, with particularly large differences in the Ebro region. This is due to variations in CHI (displayed as isolines), which is larger (smaller) in the southern (northern) Peninsula. June and September present somehow similar patterns but with lower differences in the south, with the exception over Ebro in September, where FWI is substantially larger than FWIe.

When examining the future projections for FWI, the most substantial increases in the number of extreme FWI days can be found from mid-century onwards for RCP4.5 and RCP8.5 (**Fig. 3**).

Here, changes in number of extreme FWI days surpass 100 % in many regions, starting in the north-western and central regions for RCP4.5 mid-century (with most of the remaining peninsula surpassing 50% of increase in the number of extreme FWI days). Changes larger than 100 % then spread to southern and eastern Iberia in 2071–2100 with RCP4.5, and 2041–2070 with RCP8.5, and finally occupying all the territory in 2071–2100 with RCP8.5. It is worth noticing that the larger increases are observed in the north-western region, with anomalies of more than 45 days, which corresponds to an increase of almost 5 times the historical number of extreme FWI days. Indeed, this implies that the north-western region of Iberia may have a minimum of 57 (45 + 12) days of extreme FWI days in the extended summer JJAS in 2071–2100, i.e., near halve of the 4-month summer period considered. Conversely, northern, eastern, and southern coastal regions for RCP2.6 over all periods, and the 2011–2040 over the three RCPs, show virtually non-existent changes

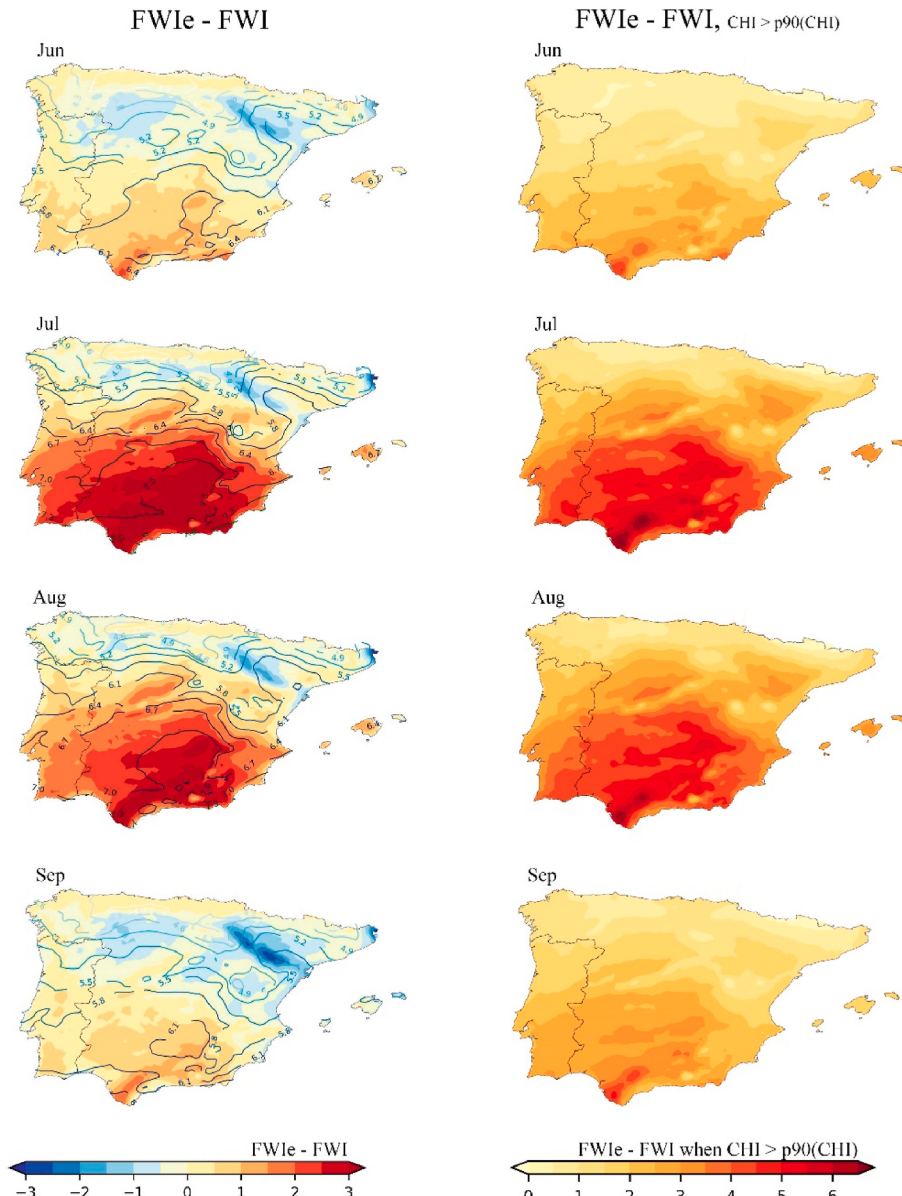


Fig. 2. Ensemble mean differences of the monthly average 90th percentile for the historical period (1971–2000) using a 5-day moving window of FWIe – FWI (left) considering all values of CHI and (right) only considering cases where CHI is larger than its 90th percentile. Contours represent the CHI spatial distribution.

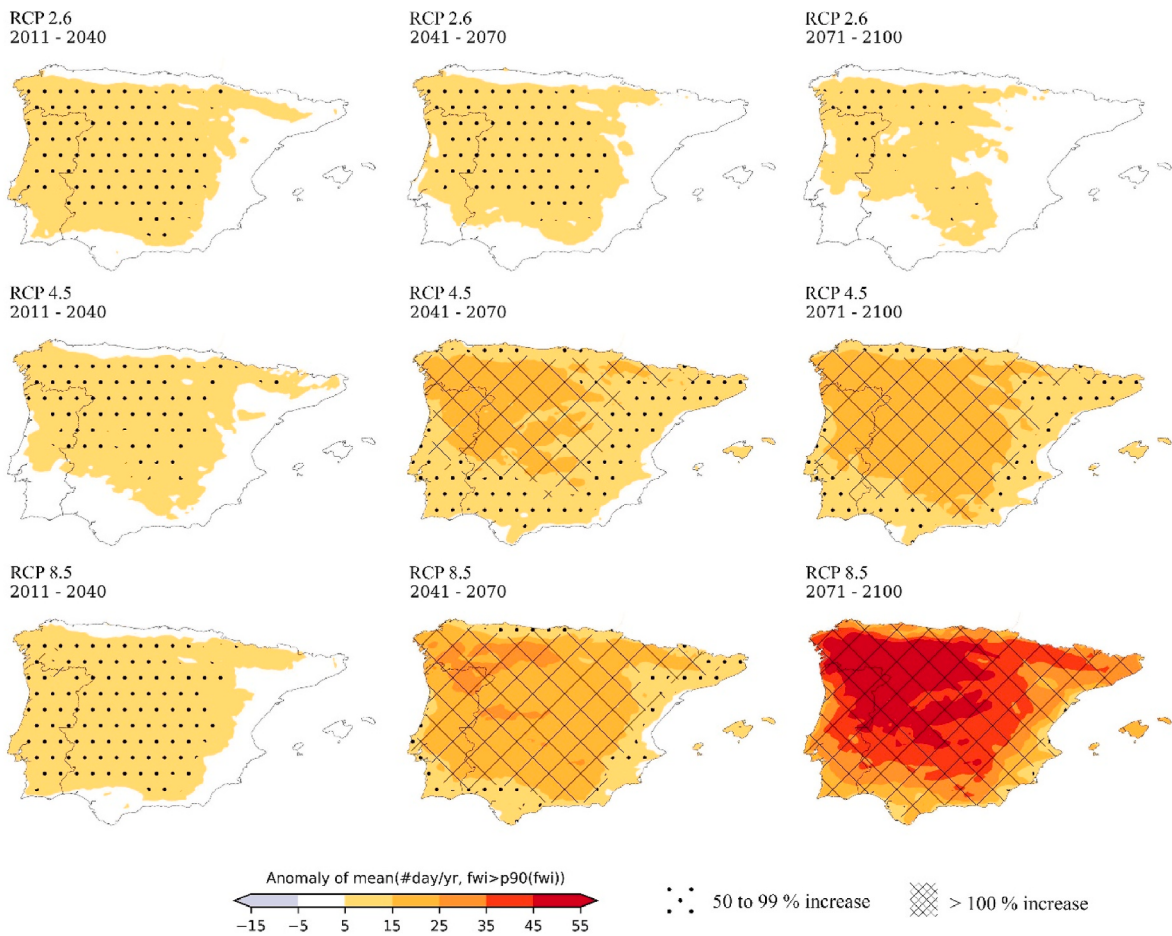


Fig. 3. Anomalous number of days with extreme fire danger measured with FWI per season (JJAS) for (left column) 2011–2040, (central column) 2041–2070, and (right column) 2071–2100 following (top row) RCP 2.6, (middle row) 4.5, and (bottom row) 8.5. Dots indicate an increase between 50 and 99 % relative to the historical period and diagonal grid indicates an increase of more than 100 % of days with extreme fire danger.

(between –5 and 5 days). Nevertheless, for the 2011–2040 period and the RCP2.6, results show already several regions where the increase surpasses 50% of historical extreme FWI days (i.e., an increase of at least 6 extreme FWI days).

Fig. 4 shows equivalent results for FWIe, with a similar behavior to FWI. However, the increase in the number of days with high fire danger by FWIe are slightly smaller than those given by FWI. The extended summer aggregated results for the anomaly of extreme FWI and FWIe days does not explicit the months where this increase may be pivotal.

Hence, Fig. 5 shows the anomaly but this time by spatially aggregating in pyro-regions and separating the individual JJAS months. The month with larger anomalies changes according to the four pyro-regions considered. For the NW pyro-region, the results for RCP4.5 and RCP8.5 show similar anomalies in JJA, with an average of more 5 (4.6) and 11.4 (10.4), respectively, of extreme FWI (FWIe) days per month, at the end of the century. The SW pyro-region shows a different behavior with June being the month with larger anomalies of extreme FWI days: 4.6 and 13.0 for RCP4.5 and RCP8.5, respectively, at the end of the century; and FWIe days: 4.2 and 12.1 for RCP4.5 and RCP8.5, respectively, at the end of the century, then progressively decreasing in the subsequent months. The E pyro-region shows a similar behavior to that of SW, having lower absolute values of anomaly (anomaly of days at end of century vary between 5.2 and 8.5 for RCP8.5 for FWI and 4.5 and 7.9 for RCP8.5 for FWIe). Finally, the N pyro-region shows alike results as those from NW, with the difference that June shows lower anomalies than July and August. For the 4 pyro-regions, September is consistently the month with lower anomalies, and projections following the RCP2.6 scenario show rather small anomalies without a strong signal distinguishing the

months and the different periods.

Fig. 6 shows a simple distributional behavior of the multi-model ensemble of FWI and FWIe for the 4 pyro-regions pre-defined of the Iberian Peninsula, focusing on the evolution of the values over the historical and three future periods of study, and considering the three RCPs. The distributions are shown separately for each individual month of the extended summer as previously defined: June, July, August, and September. As expected, pyro-regions located in the northern (NW, N) peninsula show lower absolute values of FWI and FWIe when compared with southernmost pyro-regions (SW and E pyro-regions). The increase in absolute values of these indices from June to August, and the decrease in September is clearly visible. Results presented in Fig. 6 show that values of FWI and FWIe do not considerably change for RCP2.6 over all pyro-regions/months but display a steep increase towards the end-of-century period for both RCP4.5 and RCP8.5. For the latter, differences between historical and end-of-century are larger, as expected. As an example, July shows an increase of the median from ~10 to 20 in NW, ~30 to 40 in SW, ~20 to 30 in E, and ~5 to 12 in N for both FWI and FWIe. Differences between the boxplots of the two fire weather indices are notorious when analyzing the medians and extremes. Generally, FWIe presents lower median values than FWI but a larger range between the 10th and 90th percentiles. Differences between FWI and FWIe are better described when looking at empirical cumulative distribution functions (CDFs) as shown in Figure S3 for both variables, considering the different periods, RCPs, and months, with bins of 5 units from 0 to 80. Fig. 7 displays the differences between the CDFs of FWIe and FWI (FWIe – FWI). Two examples are selected to illustrate this analysis, one with positive CDF differences, and the other with negative differences in

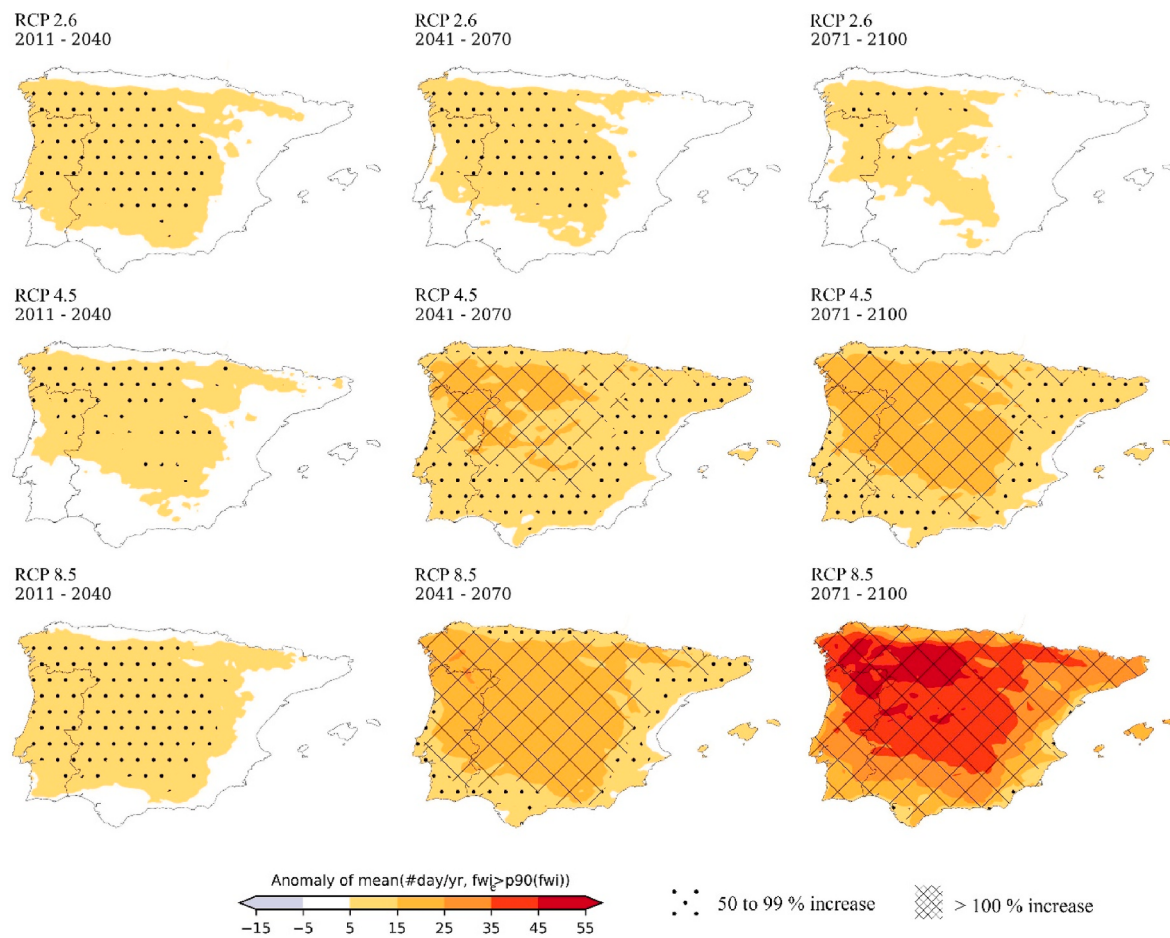


Fig. 4. Anomalous number of days with extreme fire danger measured with FWIe per season (JJAS) for (left column) 2011–2040, (central column) 2041–2070, and (right column) 2071–2100 following (top row) RCP 2.6, (middle row) 4.5, and (bottom row) 8.5. Dots indicate an increase between 50 and 99 % relative to the historical period and diagonal grid indicates an increase of more than 100 % of days with extreme fire danger.

the CDF values. These are marked as Ex.1 and Ex.2, respectively, in the panel relative to the SW pyro-region in August for the historical period (panel relative to 2011–2040). The selected positive case is situated in the meteorological fire danger class of 15–20, where there is a probability of 22 (24) % (supplementary material, Figure S3) that FWI (FWIe) takes a value belonging to that or lower fire danger classes. The negative case is selected in the 45–50 class of fire danger, and here there is a probability of 92 (90) % (supplementary material, Figure S3) that FWI (FWIe) take a value on that or lower classes. In the former case, the probability of having lower fire danger values is higher for FWIe than FWI. Conversely, the latter case indicates that FWIe is more likely to occur in higher danger classes than FWI. Hence, the general shape of the curves in Fig. 7, especially in southern regions and less notoriously in July and August in northern regions, agrees with Fig. 6. Indeed, lower, and higher extremes of FWIe tend to occur more frequently than FWI, whereas FWI tend to be more frequent for mid-range values. For all pyro-regions it is possible to observe a future shift of the FWI and FWIe CDFs to the right (supplementary material, Figure S3), which is more evident for RCP8.5 at the end of the XXI century. Nevertheless, this shift may also be found at early and mid-century periods. Examples are the month of June in SW for mid-century (supplementary material, Figure S3), where a substantial shift is already present for RCP4.5 and RCP8.5 (supplementary material, Figure S3). The shift to the right of the corresponding FWIe – FWI curves (Fig. 7) is also conspicuous. Once again this is more noticeable for RCP4.5 and RCP8.5, and for the mid- and end-century. This shift implies that the probability of having larger values of fire danger in the future is more likely (see Fig. 7).

4. Discussion

Intense summer surface heating over land generally favors the development of a thermal low over the central Iberian Peninsula (Hoinka and De Castro 2003). This area is characterized by a semi-arid climate, in which the surface evaporation is reduced, and by the relatively high altitudes of the central Iberian plateau (Gaertner et al., 1993). Although the Iberian summer thermal low has shallow convection forms, there is usually no association with the occurrence of precipitation (Trigo et al., 2002). The frequent occurrence of a thermal low during the months of July and August may justify the larger values of CHI in Fig. 2 and the corresponding larger differences between FWIe and FWI over south-central region of Iberian Peninsula, due to the high instability associated. Nonetheless, the thermal circulation generates strong pressure gradients forcing low-level winds, such as sea breezes, to blow from coast inland, being stronger as the low pressure intensifies (Portela and Castro, 1996). In river valleys and mountain passes, an enhancing of these winds occurs as a result of a channeling effect. The strengthening and channeling of the winds from the Mediterranean provides the entrance of warm and humid air into the north-eastern Iberian Peninsula, especially into the Mid Ebro Valley, contributing significantly to the local water balance over the north-eastern mountainous region during summer (Gaertner et al., 2001). A significant part of the total annual precipitation over the Ebro basin occurs during autumn, being dominant the stratiform rainfall type, which is less unstable than convective type (Iturrioz et al., 2007; Martin-Vide and Lopez-Bustins, 2006). This is a possible explanation for why FWI is substantially higher than FWIe over the Ebro basin, but a more thorough

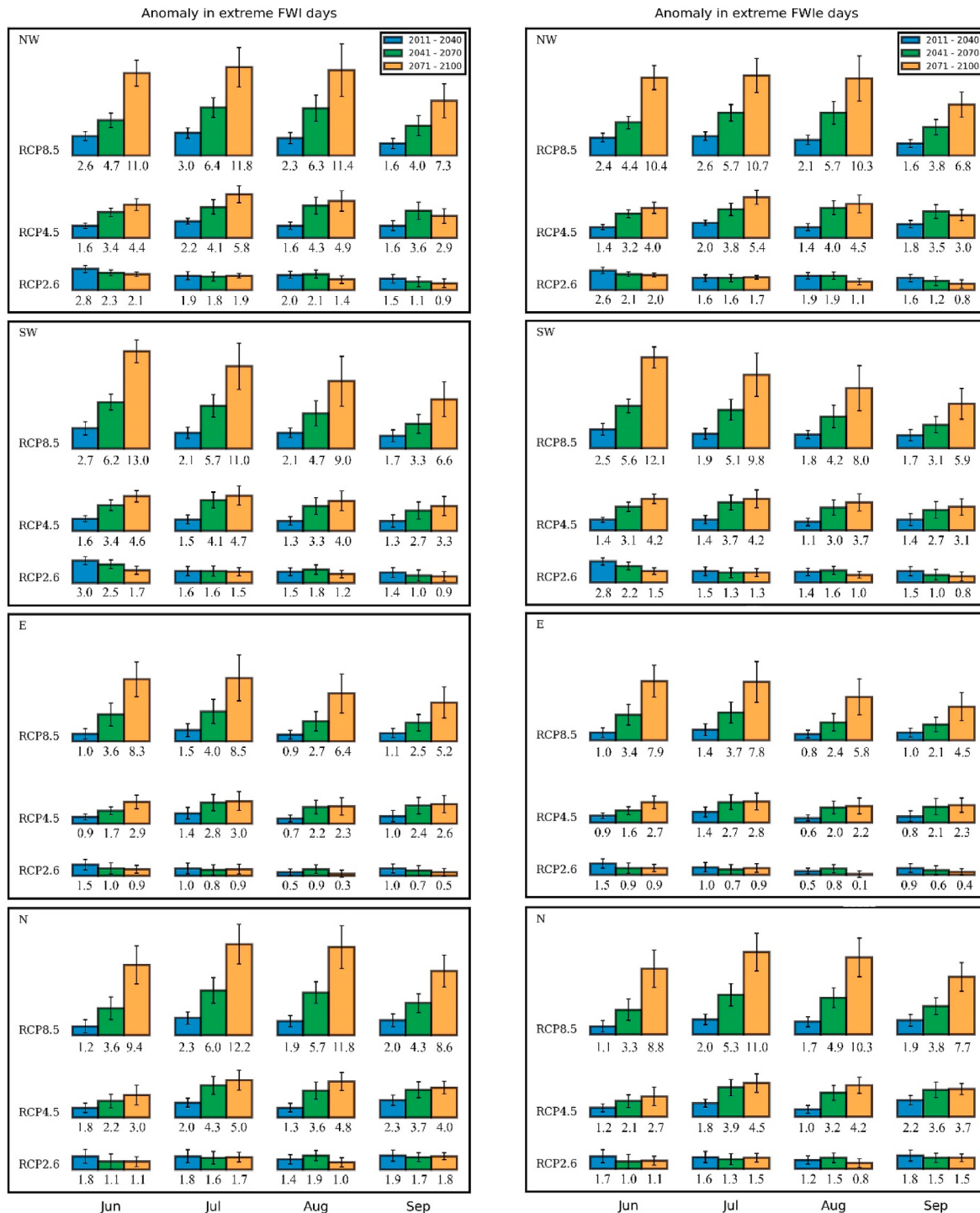


Fig. 5. Spatial mean of the anomalous number of days per month (JJAS) with extreme fire danger for NW, SW, N, and E regions (top to bottom), and for FWI and FWIe (left to right). Bar plots in blue, green, and orange represent 2011–2040, 2041–2070, and 2071–2100, respectively. The value below the bar is the spatial mean of days. The whisker represents the standard deviation. (For interpretation of the references to colour in this figure legend, the reader is referred to the Web version of this article.)

future research on this topic should be pursued.

The number of summer fire extreme danger days is projected to increase significantly in the future, with the largest anomalies relative to the historical period consistently found in the NW pyro-region with propensity to extend towards the Iberian central region. These results agree with those obtained by Calheiros et al. (2021) that also rely on information from CORDEX RCMs and address the projected northward extension of the SW pyro-region. The study also points to meteorological

fire weather danger values increasing considerably when going from historical to future scenarios, especially in late spring and early autumn. However, the authors did not consider fire danger projections driven by the strongly mitigated RCP2.6 scenario. Our results are also in line with those from other studies that project FWIs into the future with different RCMs ensemble architectures, different periods, and different scenarios (Bedia and Herrera, 2013; Bedia et al., 2014; Camia et al., 2017; Moriondo et al., 2006). Here, we showed that besides the increase in extreme

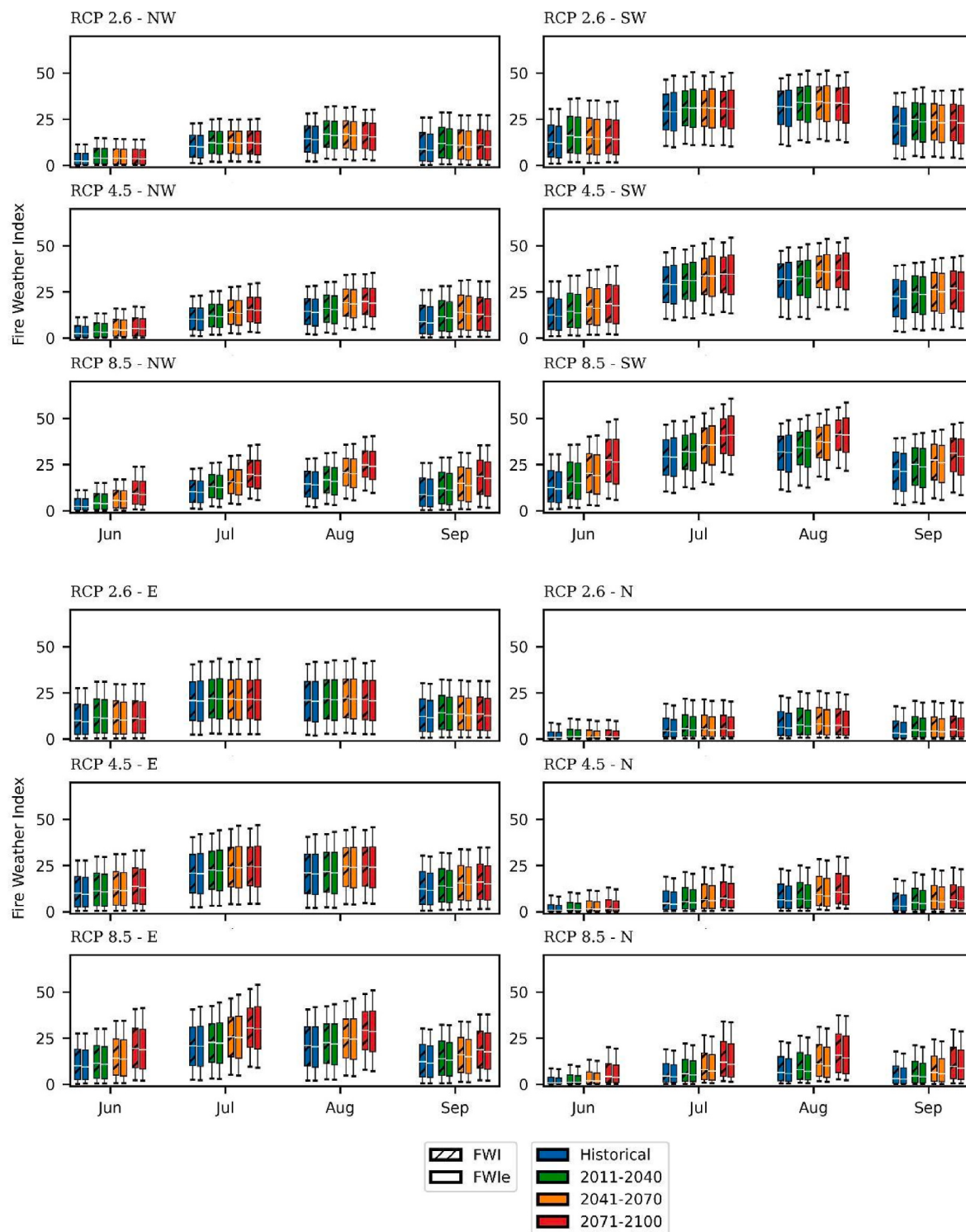


Fig. 6. Monthly (JJAS) comparison of the distribution of FWI (solid with dashes) and FWIe (solid) for historical (blue), 2011–2040 (green), 2041–2070 (orange), and 2071–2100 (red) for the NW (top left), SW (top right), E (bottom left), and N (bottom right). For each region RCP 2.6, RCP 4.5, and RCP 8.5 are shown (top to bottom). Boxes represent interquartile distance, whiskers represent the 10th and 90th percentiles, and white dash represents the median. (For interpretation of the references to colour in this figure legend, the reader is referred to the Web version of this article.)

danger days in July and August, June also displays relevant increases in most of the pyro-regions. In this case, the SW shows the most striking behavior of fire danger in June, being even larger than the increases in the traditional fire season months of July and August. This is also in agreement with results by (Peña-Ortiz et al., 2015), which state that, as a result from the ongoing changing climate, summers are becoming longer

and with an earlier onset (June). Other work also points to the increase in burned area related with heatwaves in these regions in month of June (Bento et al., 2022). Recent rare destructive events, such as the June 2017 fires in central Portugal (Sánchez-Benítez et al., 2018; Turco et al., 2019), already support this premise. The disentanglement of variables such as precipitation, minimum and maximum temperature, and wind

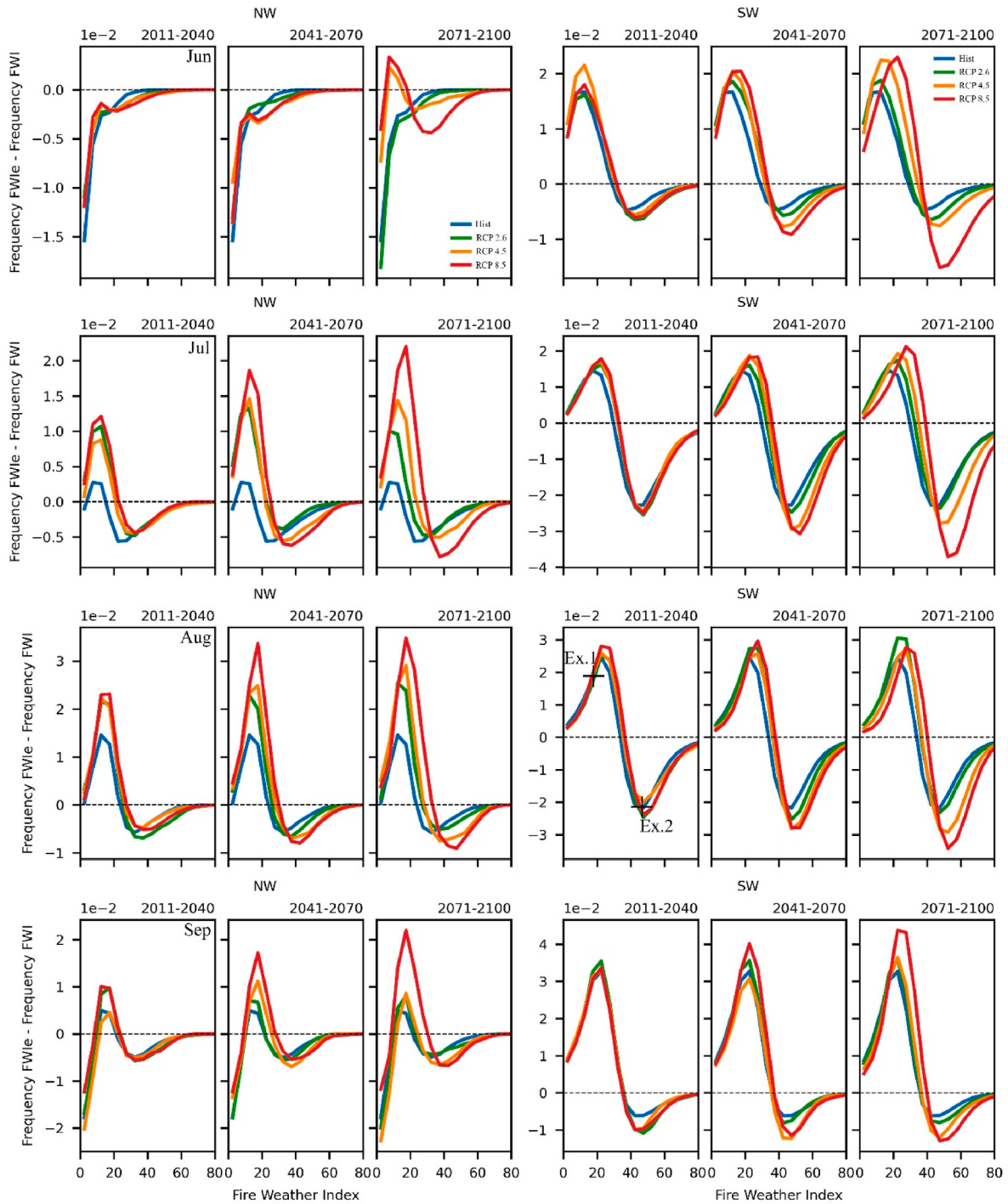


Fig. 7. Differences between CDFs of FWIe and FWI (FWIe – FWI) for NW (left) and SW (right) for the months of JJAS (top to bottom). Ex. 1 and Ex.2 are examples explained in the text. a. Differences between CDFs of FWIe and FWI (FWIe – FWI) for E (left) and N (right) for the months of JJAS (top to bottom).

speed may also be addressed. In that sense, Soares et al. (2017a) showed that for Portugal in summer (JJA) total accumulated precipitation is expected to decrease up to 50 % in 2071–2100; daily maximum temperature is expected to increase, especially in the northern region, where anomalies may peak at + 6 °C in the late century (Cardoso et al., 2019); daily minimum temperature follows a similar pattern but peaking at anomalies of +5 °C in the northern region (Cardoso et al., 2019); and daily mean wind speed at 10 m may increase up to + 0.6 m/s (Nogueira et al., 2019), in agreement with the RCP8.5.

Results presented in this study show a clear shift to the right of the

CDFs of FWIe – FWI, which implies that the probability of having values on the higher classes of fire danger in the future is more likely. This is especially noticeable in scenarios without greenhouse gas emissions mitigation (RCP8.5), but also in some regions with scenarios that include some mitigation (RCP4.5) or strong mitigation (RCP2.6). These findings underscore the importance of incorporating atmospheric instability into the formulation of a fire danger index, particularly in the context of monitoring convective wildfires. Convective wildfires represent dynamic and unpredictable events characterized by the confluence of intense atmospheric instability and an abundance of accumulated

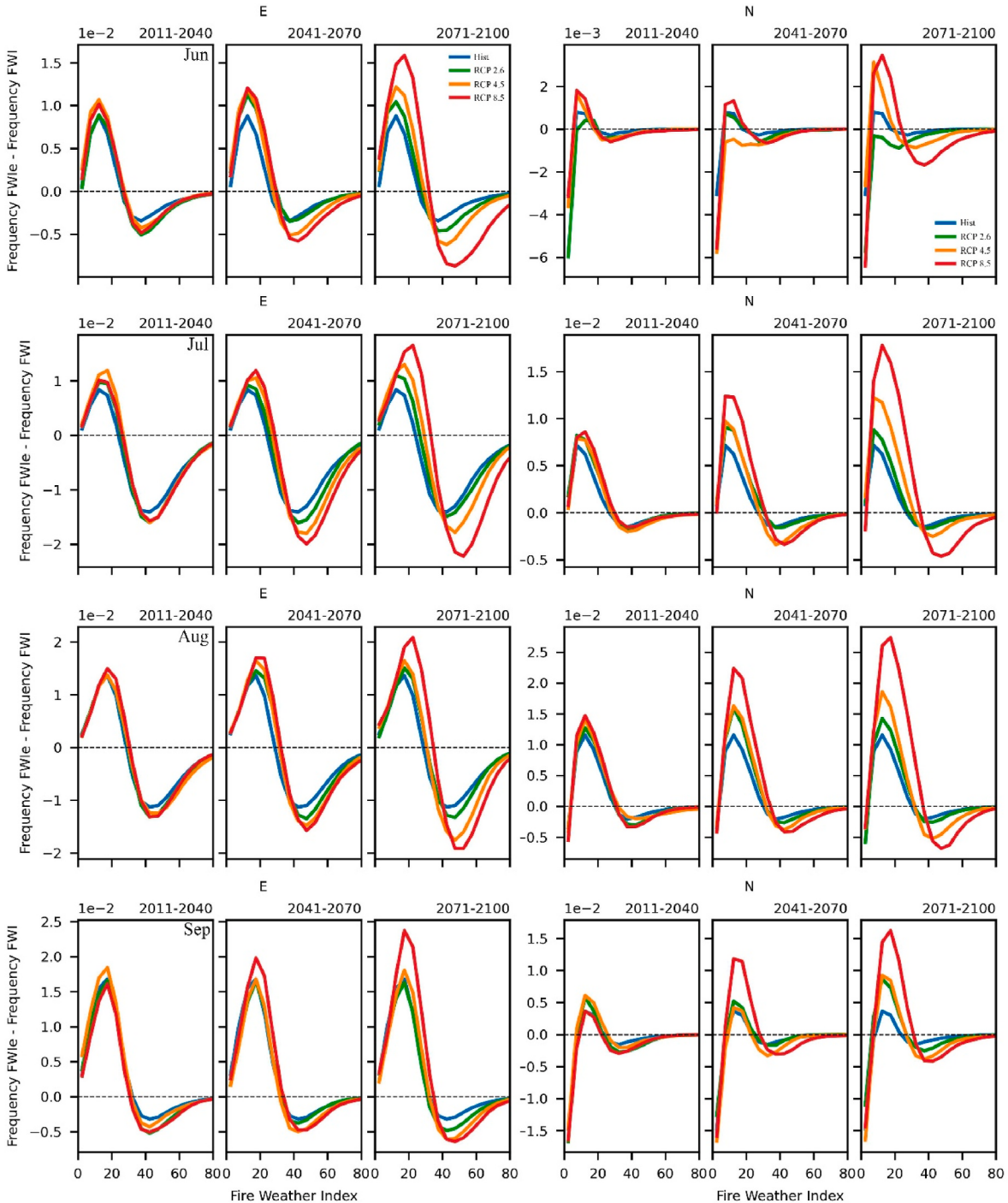


Fig. 7. (continued).

fuel, as observed by Lareau and Clements (2017). Pinto et al. (2020) further elucidated the critical role of the Fire Weather Index enhanced with instability (FWIe) on days marked by convective activity, such as those witnessed during the 2018 Monchique wildfire in southern Portugal and the 2005 Guadalajara wildfire in central Spain. Results from these studies highlight the disparities between the standard Fire Weather Index (FWI) and the enhanced FWIe, with discrepancies of up to 10 points in some instances. The SW and E clusters are those more affected by atmospheric instability and are the ones where FWIe in the future shows larger differences in CDFs to FWI (negative peaks for high FWI classes in Fig. 7). This is especially noticeable in July and August in the SW region for RCP8.5 at the end of the century since there is an

expected strengthening in the thermal low over central Iberia in the future due to local warming (Cardoso et al., 2016; Soares et al., 2017c). Conversely, N and NW clusters show larger differences in CDFs between FWIe and FWI for lower fire danger classes (positive peaks for low fire danger classes in Fig. 7). This means that there is a tendency to have more values of FWIe in lower classes, i.e., lower values of atmospheric instability in the future, especially in July and August for RCP8.5 in the end of the century. This may be related to future changes in the thermal low characteristics.

Although FWI and FWIe are solely driven by meteorological variables, these results point to a substantial problem of wildfire adaptation and mitigation to climate change in the region. However, it is worth

noticing that with a strong mitigation scenario, such as RCP2.6, projections of fire danger are not as drastic as those projected with a no mitigation scenario, such as RCP8.5. Nevertheless, even meteorological fire danger projections in the context of RCP2.6 show a slight increase of extreme danger days. Hence, adaptation strategies to prevent large ecological, economical, and human losses must be developed by taking several scenarios into account. Of course, the presence of biomass and ignition are critical variables without which a fire cannot occur. For example, it ought to be noted that the occurrence of an extreme wildfire, such as the one from October 2017 in Portugal, should be analysed from the compound perspective (Ramos et al., 2023): the passage of hurricane Ophelia off the coast of Portugal was responsible for exceptional meteorological conditions such as the elevated atmospheric instability (Pinto et al., 2018), associated with a prolonged drought that led to pre-conditioned cumulative hydric stress of the vegetation (García-Herrera et al., 2019), and the anthropogenic factor that led to an extremely large number of negligent ignitions (Guerreiro et al., 2018). Forthcoming work may focus on the relation of vegetation and ignition probabilities, for example by using the new CMIP6 models which have a dynamical vegetation component.

With this study we present a comprehensive analysis of future fire danger in the Iberian Peninsula, taking advantage of indices such as FWI, and the state-of-the-art FWIe. The latter was recently shown to be an important asset for fire danger monitoring in the region of study (Pinto et al., 2020). Furthermore, the methods used in this study include the use of a state-of-the-art high quality weighted multi-model ensemble developed specifically for the region (Lima et al., 2023a, 2023b) and the use of three RCPs from strong to no mitigation and three projected periods (2011–2040, 2041–2070, and 2071–2100). The use of a weighted multi-model ensemble approach led to a better ensemble performance during present climate, helped constrain the uncertainty of climate modelling, and helped achieve more accurate regional climate projections (Lima et al., 2023a; Christensen et al., 2010; Eyring et al., 2019; Knutti et al., 2017; Sanderson et al., 2017). However, we acknowledge that this study presents some caveats. Indeed, a major limitation is the impossibility to use variables at noon with EURO-CORDEX RCMs, where variables are usually available at a daily scale. A previous work (Herrera et al., 2013) advocated caution when using daily means instead of instantaneous values at noon, arguing that fire danger extremes cannot be reliably converted from daily means into instantaneous values in order to accommodate magnitude and spatial patterns of FWI. The same work pointed out that daily mean data lead to systematic negative biases of fire danger calculations, leading to an underestimation of fire danger (Bedia and Herrera, 2013). Bedia et al. (2014) analysed the use of maximum temperature and minimum relative humidity as proxy variables of the instantaneous input data at noon (available in ENSEMBLES RCMs), concluding that their use together with daily mean variables for the remaining inputs provides realistic estimates of fire danger scenarios using the ENSEMBLES RCMs in current climate. A future similar analysis based on information from EURO-CORDEX RCMs will allow defining the best proxies to both FWI and FWIe. It is also worth emphasizing that this work deals with meteorological fire danger alone, and therefore, it does not include any variable linked with the occurrence of fires (e.g., Fire Radiative Power) that may characterize fire activity into the future. Such endeavor must be tackled in a future assessment linking meteorological fire danger (and its climate change evolution) with ignitions and burned area, for example following the works by DaCamara et al. (2023) or Nunes et al. (2023). Such work should be key to the development of mitigation and adaptation measures in the region. Nevertheless, in terms of designing storylines for adaptation strategies in Portugal and Spain, results from the present study may be considered a relevant regional starting point. Furthermore, it is relevant to stress that in this study RCMs are forced with GCMs from CMIP5, with simulations based on RCPs. In the near future, regional simulations based on CMIP6 will be available with Shared Socioeconomic Pathways (SSPs), which may be an important asset to study the impact of future projections of fire danger in

the population.

5. Final remarks

This investigation was performed in the framework of the National Roadmap for Adaptation XXI - Portuguese Territorial Climate Change Vulnerability Assessment for XXI Century (RNA2100). This project's pillar objectives include the development and definition of adaptation strategies for Portugal, where the choice of climate models, multi-model ensemble, and regionalization are key components. Here, we present a continuation of previous works related with the assessment and characterization of climate change impacts on a number of main climate variables and extremes from highly-to non-mitigated emission scenarios based on a multi-variable constrained ensemble. In the scope of this project, climate change projections of FWI and the new state-of-the-art enhanced FWIe were here compared. A multi-model ensemble with 13 RCMs was used for historical (1971–2000) and three future periods (2011–2040, 2041–2070, 2071–2100) in agreement with RCP2.6, RCP4.5, and RCP8.5. Results indicate that summer days with extreme FWI and FWIe are expected to substantially increase in the future for scenarios RCP4.5 and RCP8.5, with an extension of the danger period to June and, in lower magnitude, to September. The north-western region of Iberia, encapsulating the north of Portugal and the north-western-to-central Spain, are the regions with larger increases in meteorological fire danger. This may lead to especially dramatic consequences since these regions are vastly forested. Nevertheless, projections point to little future fire danger increases in the context of RCP2.6, which in comparison with RCP4.5 and RCP8.5 will require less adaptation needs. A sensitivity analysis to forest management and their vulnerability to wildfires is an important step that needs to take place next. Future work exploring the relationship between meteorological indices such as FWI and FWIe and vegetation is crucial. However, the issue of vegetation projections and how to include them in the RCMs needs further analysis. The new CMIP6 projections, with dynamic vegetation, may be an important asset for such studies. Incorporated in the RNA2100 project, this work aims at being a baseline to timely prepare forest wildfire adaptation measures, and to further translate into storylines articulated and integrated with the stakeholders' and policymakers' point-of-view.

CRediT authorship contribution statement

Virgilio A. Bento: Conceptualization, Methodology, Validation, Formal analysis, Writing – original draft, Visualization. **Daniela C.A. Lima:** Methodology, Validation, Formal analysis, Writing – review & editing, Visualization. **Luana C. Santos:** Validation, Writing – review & editing. **Miguel M. Lima:** Validation, Writing – review & editing. **Ana Russo:** Conceptualization, Writing – review & editing. **Carlos C. DaCamara:** Conceptualization, Methodology, Formal analysis, Writing – review & editing. **Ricardo M. Trigo:** Methodology, Writing – review & editing, Conceptualization, Validation, Writing – review & editing. **Pedro M.M. Soares:** Conceptualization, Validation, Writing – review & editing.

Declaration of competing interest

The authors declare that they have no known competing financial interests or personal relationships that could have appeared to influence the work reported in this paper.

Data availability

Data will be made available on request.

Acknowledgements

This work was funded by the Portuguese Fundação para a Ciência e a

Tecnologia (FCT) I.P./MCTES through national funds (PIDDAC) – UIDB/50019/2020, the project “Forecasting fire probability and characteristic for a habitable pyroenvironment (Fire-Cast)” under grant no. PCIF/GRF/0204/2017, and project DHEFEUS - 2022.09185. PTDC. The authors also acknowledge EEA-Financial Mechanism 2014–2021 and the Portuguese Environment Agency through Pre-defined Project-2 National Roadmap for Adaptation XXI (PDP-2) for the data’s provided. D.C.A.L. is supported by the Scientific Employment Stimulus 5th edition from Fundação para a Ciência e a Tecnologia (FCT, 2022.03183.CEECIND). A.R. has been supported by the Fundação para a Ciência e a Tecnologia (FCT) I.P./MCTES through national funds (PIDDAC, grant no. UIDB/50019/2020 to Instituto Dom Luiz; project DHEFEUS, <https://doi.org/10.54499/2022.09185.PTDC>; COMPLEX, 2022.01167.CEECIND). L.C.S. would like to acknowledge the project “CEASEFIRE: Envio e disseminação de alertas automatizados de gestão de perigo meteorológico de incêndio”, financed by The Navigator Company. M.M.L. would like to acknowledge the project “Extração de dados por chamada de url com parâmetros - CEASEFIRE”, financed by E-REDES. We also acknowledge the World Climate Research Programme’s Working Group on Regional Climate, and the Working Group on Coupled Modelling, former coordinating body of CORDEX and responsible panel for CMIP5. We also thank the climate modelling groups for producing and making available their model output. We also acknowledge the Earth System Grid Federation infrastructure an international effort led by the U.S. Department of Energy’s Program for Climate Model Diagnosis and Intercomparison, the European Network for Earth System Modelling and other partners in the Global Organisation for Earth System Science Portals (GO-ESSP).

Appendix A. Supplementary data

Supplementary data to this article can be found online at <https://doi.org/10.1016/j.wace.2023.100623>.

References

- Alessandri, A., de Felice, M., Zeng, N., Mariotti, A., Pan, Y., Cherchi, A., Lee, J.Y., Wang, B., Ha, K.J., Ruti, P., Artale, V., 2014. Robust assessment of the expansion and retreat of Mediterranean climate in the 21st century. *Sci. Rep.* 4, 1–8. <https://doi.org/10.1038/srep07211>.
- Augusto, S., Ratola, N., Tarín-Carrasco, P., Jiménez-Guerrero, P., Turco, M., Schuhmacher, M., Costa, S., Teixeira, J.P., Costa, C., 2020. Population exposure to particulate-matter and related mortality due to the Portuguese wildfires in October 2017 driven by storm Ophelia. *Environ. Int.* 144, 106056 <https://doi.org/10.1016/j.envint.2020.106056>.
- Bedia, J., Herrera, S., 2013. SHORT COMMENT on NHESSD article entitled: Sensitivity and evaluation of current fire risk and future projections due to climate change: the case study of Greece (by Karali et al.). <https://doi.org/10.1007/s10584-012-0667-2>.
- Bedia, J., Herrera, S., Camia, A., Moreno, J.M., Gutiérrez, J.M., 2014. Forest fire danger projections in the Mediterranean using ENSEMBLES regional climate change scenarios. *Clim. Change* 122, 185–199. <https://doi.org/10.1007/S10584-013-1005-Z>.
- Bento, V.A., Russo, A., Gouveia, C.M., Dacamara, C.C., 2022. Recent change of burned area associated with summer heat extremes over Iberia. *Int. J. Wildland Fire* 31, 658–669. <https://doi.org/10.1071/WF21155>.
- Boberg, F., Berg, P., Theijll, P., Gutowski, W.J., Christensen, J.H., 2009. Improved confidence in climate change projections of precipitation evaluated using daily statistics from the PRUDENCE ensemble. *Clim. Dynam.* 32, 1097–1106. <https://doi.org/10.1007/s00382-008-0446-y>.
- Boer, M.M., Resco de Dios, V., Bradstock, R.A., 2020. Unprecedented burn area of Australian mega forest fires. *Nat. Clim. Change* 10, 171–172. <https://doi.org/10.1038/s41558-020-0716-1>.
- Bowman, D.M.J.S., Kolden, C.A., Abatzoglou, J.T., Johnston, F.H., van der Werf, G.R., Flannigan, M., 2020. Vegetation fires in the anthropocene. *Nat. Rev. Earth Environ.* 11 (1), 500–515. <https://doi.org/10.1038/s43017-020-0085-3>.
- Brunner, L., Lorenz, R., Zumwald, M., Knutti, R., 2019. Quantifying uncertainty in European climate projections using combined performance-independence weighting. *Environ. Res. Lett.* 14, 124010 <https://doi.org/10.1088/1748-9326/ab492f>.
- Calheiros, T., Pereira, M.G., Nunes, J.P., 2021. Assessing impacts of future climate change on extreme fire weather and pyro-regions in Iberian Peninsula. *Sci. Total Environ.* 754, 142233 <https://doi.org/10.1016/J.SCITOTENV.2020.142233>.
- Camia, A., Libertà, G., San-Miguel-Ayanz, J., 2017. Modeling the impacts of climate change on forest fire danger in Europe: sectorial results of the PESETA II Project. *Publ. Off.* 24. <https://doi.org/10.2760/768481>.
- Cardoso, R.M., Soares, P.M.M., 2022. Is there added value in the EURO-CORDEX hindcast temperature simulations? Assessing the added value using climate distributions in Europe. *Int. J. Climatol.* <https://doi.org/10.1002/joc.7472>.
- Cardoso, R.M., Soares, P.M.M., Lima, D.C.A., Miranda, P.M.A., 2019. Mean and extreme temperatures in a warming climate: EURO CORDEX and WRF regional climate high-resolution projections for Portugal. *Clim. Dynam.* 52, 129–157. <https://doi.org/10.1007/s00382-018-4124-4>.
- Cardoso, R.M., Soares, P.M.M., Lima, D.C.A., Semedo, A., 2016. The impact of climate change on the Iberian low-level wind jet: EURO-CORDEX regional climate simulation. *Tellus, Series A: Dynamic Meteorology and Oceanography* 68, 29005. <https://doi.org/10.3402/tellusa.v68.29005>.
- Careto, J.A.M., Soares, P.M.M., Cardoso, R.M., Herrera, S., Gutiérrez, J.M., 2022a. Added value of EURO-CORDEX high-resolution downscaling over the Iberian Peninsula revisited – Part 1: precipitation. *Geosci. Model Dev. (GMD)* 15, 2635–2652. <https://doi.org/10.5194/gmd-15-2635-2022>.
- Careto, J.A.M., Soares, P.M.M., Cardoso, R.M., Herrera, S., Gutiérrez, J.M., 2022b. Added value of EURO-CORDEX high-resolution downscaling over the Iberian Peninsula revisited – Part 2: max and min temperature. *Geosci. Model Dev. (GMD)* 15, 2653–2671. <https://doi.org/10.5194/gmd-15-2653-2022>.
- Carvalho, A., Flannigan, M.D., Logan, K.A., Gowman, L.M., Miranda, A.I., Borrego, C., 2009. The impact of spatial resolution on area burned and fire occurrence projections in Portugal under climate change. *Clim. Change* 98, 177–197. <https://doi.org/10.1007/s10584-009-9667-2>.
- Casanueva, A., Kotlarski, S., Herrera, S., Fernández, J., Gutiérrez, J.M., Boberg, F., Colette, A., Christensen, O.B., Goergen, K., Jacob, D., Keuler, K., Nikulin, G., Teichmann, C., Vautard, R., 2016. Daily precipitation statistics in a EURO-CORDEX RCM ensemble: added value of raw and bias-corrected high-resolution simulations. *Clim. Dynam.* 47, 719–737. <https://doi.org/10.1007/s00382-015-2865-x>.
- Christensen, O.B., Drews, M., Christensen, J.H., Dethloff, K., Ketelsen, K., Hebestadt, I., Rinke, A., 2007. The HIRHAM Regional Climate Model Version 5 (beta). *Tech. Rep. 06-17*, 1–22.
- Christensen, J.H., Kjellström, E., Giorgi, F., Lenderink, G., Rummukainen, M., 2010. Weight assignment in regional climate models. *Clim. Res.* 44, 179–194. <https://doi.org/10.3354/cr00916>.
- Colin, J., DéQué, M., Radu, R., Somot, S., 2010. Sensitivity study of heavy precipitation in Limited Area Model climate simulations: Influence of the size of the domain and the use of the spectral nudging technique. *Tellus Ser. A Dyn. Meteorol. Oceanogr.* 62, 591–604. <https://doi.org/10.1111/j.1600-0870.2010.00467.x>.
- DaCamara, C.C., Calado, T.J., Ermida, S.L., Trigo, I.F., Amraoui, M., Turkman, K.F., 2014. Calibration of the Fire Weather Index over Mediterranean Europe based on fire activity retrieved from MSG satellite imagery. *Int. J. Wildland Fire* 23, 945–958. <https://doi.org/10.1071/WF13157>.
- DaCamara, C.C., Libonati, R., Nunes, S.A., de Zea Bermudez, P., Pereira, J.M.C., 2023. Global-scale statistical modelling of the radiative power released by vegetation fires using a doubly truncated lognormal body distribution with generalized Pareto tails. *Phys. A Stat. Mech. its Appl.* 625, 129049 <https://doi.org/10.1016/J.PHYSA.2023.129049>.
- Diffenbaugh, N.S., Giorgi, F., 2012. Climate change hotspots in the CMIP5 global climate model ensemble. *Clim. Change* 114, 813–822. <https://doi.org/10.1007/s10584-012-0570-x>.
- Dowdy, A.J., Ye, H., Pepler, A., Thatcher, M., Osbrough, S.L., Evans, J.P., Di Virgilio, G., McCarthy, N., 2019. Future changes in extreme weather and pyroconvection risk factors for Australian wildfires. *Sci. Rep.* 9, 1–11. <https://doi.org/10.1038/s41598-019-46362-x>.
- Dupuy, J., luc, Farageon, H., Martin-StPaul, N., Pimont, F., Ruffault, J., Guijarro, M., Hernando, C., Madrigal, J., Fernandes, P., 2020. Climate change impact on future wildfire danger and activity in southern Europe: a review. *Ann. For. Sci.* <https://doi.org/10.1007/s13595-020-00933-5>.
- Eyring, V., Cox, P.M., Flato, G.M., Gleckler, P.J., Abramowitz, G., Caldwell, P., Collins, W.D., Gier, B.K., Hall, A.D., Hoffman, F.M., Hurtt, G.C., Jahn, A., Jones, C.D., Klein, S.A., Krasting, J.P., Kwiatkowski, L., Lorenz, R., Maloney, E., Meehl, G.A., Pendergrass, A.G., Pincus, R., Ruane, A.C., Russell, J.L., Sanderson, B.M., Santer, B.D., Sherwood, S.C., Simpson, I.R., Stouffer, R.J., Williamson, M.S., 2019. Taking climate model evaluation to the next level. *Nat. Clim. Change* 9, 102–110. <https://doi.org/10.1038/s41558-018-0355-y>.
- Faggiani, P., 2018. Estimating fire danger over Italy in the next decades. *EuroMediterr J Environ Integr* 3, 1–13. <https://doi.org/10.1007/s41207-018-0053-1>.
- Farageon, H., Pimont, F., Martin-StPaul, N., de Caceres, M., Ruffault, J., Barbero, R., Dupuy, J.L., 2020. Projections of fire danger under climate change over France: where do the greatest uncertainties lie? *Clim. Change* 160, 479–493. <https://doi.org/10.1007/s10584-019-02629-w>.
- Gaertner, M.A., Christensen, O.B., Prego, J.A., Polcher, J., Gallardo, C., Castro, M., 2001. The impact of deforestation on the hydrological cycle in the western Mediterranean: an ensemble study with two regional climate models. *Clim. Dynam.* 17, 857–873. <https://doi.org/10.1007/s003820100151>.
- Gaertner, M.A., Fernandez, C., Castro, M., 1993. A two-dimensional simulation of the Iberian summer thermal low. *Mon. Weather Rev.* 121, 2740–2756. [https://doi.org/10.1175/1520-0493\(1993\)121<2740:ATDSOT>2.0.CO](https://doi.org/10.1175/1520-0493(1993)121<2740:ATDSOT>2.0.CO).
- García-Herrera, R., Garrido-Perez, J.M., Barriopedro, D., Ordóñez, C., Vicente-Serrano, S. M., Nieto, R., Gimeno, L., Sorí, R., Yiou, P., 2019. The European 2016/17 drought. *J. Clim.* 32, 3169–3187. <https://doi.org/10.1175/JCLI-D-18-0331.1>.
- Giannakopoulos, C., le Sage, P., Bindi, M., Moriondo, M., Kostopoulou, E., Goodess, C. M., 2009. Climatic changes and associated impacts in the Mediterranean resulting from a 2 °C global warming. *Global Planet. Change* 68, 209–224. <https://doi.org/10.1016/j.gloplacha.2009.06.001>.

- Giorgi, F., Jones, C., Asrar, G., 2009. Addressing Climate Information Needs at the Regional Level: the CORDEX Framework. *WMO Bulletin*.
- Goss, M., Swain, D.L., Abatzoglou, J.T., Sarhad, A., Kolden, C.A., Williams, A.P., Diffenbaugh, N.S., 2020. Climate change is increasing the likelihood of extreme autumn wildfire conditions across California. *Environ. Res. Lett.* 15, 094016. <https://doi.org/10.1088/1748-9326/ab83a7>.
- Gouveia, C.M., Bistinas, I., Liberato, M.L.R., Bastos, A., Koutsias, N., Trigo, R., 2016. The outstanding synergy between drought, heatwaves and fuel on the 2007 Southern Greece exceptional fire season. *Agric. For. Meteorol.* 218–219, 135–145. <https://doi.org/10.1016/j.agrformet.2015.11.023>.
- Guerreiro, J., Fonseca, C., Salgueiro, A., Fernandes, P., Lopez Iglesias, E., de Neufville, R., Mateus, F., Castelnou Ribau, M., Sande Silva, J., Moura, J., Castro Rego, F., DN, C., 2018. Avaliação dos incêndios ocorridos entre 14 e 16 de outubro de 2017 em Portugal Continental. Relatório Final. Comissão Técnica Independente, Assem. da Repúbl. Lisboa.
- Haines, D.A., 1988. A lower atmospheric severity index for wildland fires. *Natl. Weather Digest* 13, 23–27.
- Herrera, S., Bedia, J., Gutiérrez, J.M., Fernández, J., Moreno, J.M., 2013. On the projection of future fire danger conditions with various instantaneous/mean-daily data sources. *Clim. Change* 118, 827–840. <https://doi.org/10.1007/s10584-012-0667-2>.
- Herrera, S., Soares, P.M.M., Cardoso, R.M., Gutiérrez, J.M., 2020. Evaluation of the EURO-CORDEX regional climate models over the Iberian peninsula: observational uncertainty analysis. *J. Geophys. Res. Atmos.* 125. <https://doi.org/10.1029/2020JD032880>.
- Hersbach, H., Bell, B., Berrisford, P., Horányi, A., Sabater, J.M., Nicolas, J., Radu, R., Schepers, D., Simmons, A., Soci, C., Dee, D., 2019. Global reanalysis: goodbye ERA-Interim, hello ERA5. *ECMWF Newsletter* 159, 17–24.
- Hoinka, K.P., de Castro, M., 2003. The Iberian Peninsula thermal low. *Q. J. R. Meteorol. Soc.* 129, 1491–1511. <https://doi.org/10.1256/qj.01.189>.
- ICNF, 2017. Relatório Provisório de Incêndios Florestais—2017. Lisboa.
- Iturrioz, I., Hernández, E., Ríbera, P., Queralt, S., 2007. Instability and its relation to precipitation over the eastern Iberian peninsula. *Adv. Geosci.* 10, 45–50. <https://doi.org/10.5194/adgeo-10-45-2007>.
- Jacob, D., 2001. A note to the simulation of the annual and inter-annual variability of the water budget over the Baltic Sea drainage basin. *Meteorol. Atmos. Phys.* 77, 61–73. <https://doi.org/10.1007/s007030170017>.
- Jacob, D., Elizalde, A., Haensler, A., Hägemann, S., Kumar, P., Podzun, R., Rechid, D., Remedio, A.R., Saeed, F., Sieck, K., Teichmann, C., Wilhelm, C., 2012. Assessing the transferability of the regional climate model REMO to different coordinated regional climate downscaling experiment (CORDEX) regions. *Atmosphere (Basel)* 3, 181–199. <https://doi.org/10.3390/atmos3010181>.
- Jacob, D., Petersen, J., Eggert, B., Alias, A., Christensen, O.B., Bouwer, L.M., Braun, A., Colette, A., Déqué, M., Georgievski, G., Georgopoulou, E., Gobiet, A., Menut, L., Nikulin, G., Haensler, A., Hempelmann, N., Jones, C., Keuler, K., Kovats, S., Kröner, N., Kotlarski, S., Kriegsmann, A., Martin, E., van Meijgaard, E., Moseley, C., Pfeifer, S., Preuschmann, S., Radermacher, C., Radtke, K., Rechid, D., Rounsevell, M., Samuelsson, P., Somot, S., Soussana, J.F., Teichmann, C., Valentini, R., Vautard, R., Weber, B., Yiou, P., 2014. EURO-CORDEX: new high-resolution climate change projections for European impact research. *Reg. Environ. Change* 14, 563–578. <https://doi.org/10.1007/s10113-013-0499-2>.
- Jacob, D., Teichmann, C., Sobolowski, S., Katragkou, E., Anders, I., Belda, M., Benestad, R., Boberg, F., Buonomo, E., Cardoso, R.M., Casanueva, A., Christensen, O.B., Christensen, J.H., Coppola, E., de Cruz, L., Davin, E.L., Dobler, A., Domínguez, M., Fealy, R., Fernandez, J., Gaertner, M.A., García-Díez, M., Giorgi, F., Gobiet, A., Goergen, K., Gómez-Navarro, J.J., Alemán, J.J.G., Gutiérrez, C., Gutiérrez, J.M., Gütterl, I., Haensler, A., Halenka, T., Jerez, S., Jiménez-Guerrero, P., Jones, R.G., Keuler, K., Kjellström, E., Knist, S., Kotlarski, S., Maraun, D., van Meijgaard, E., Mercogliano, P., Montávez, J.P., Navarra, A., Nikulin, G., de Noblet-Ducoudré, N., Panitz, H.J., Pfeifer, S., Piazza, M., Pichelli, E., Pietikäinen, J.P., Prein, A.F., Preuschmann, S., Rechid, D., Rockel, B., Romera, R., Sánchez, E., Sieck, K., Soares, P.M.M., Somot, S., Smec, L., Sorland, S.L., Termonia, P., Truhetz, H., Vautard, R., Warrach-Sagi, K., Wulfmeyer, V., 2020. Regional climate downscaling over Europe: perspectives from the EURO-CORDEX community. *Reg. Environ. Change* 20, 1–20. <https://doi.org/10.1007/s10113-020-01606-9>.
- Jones, M.W., Abatzoglou, J.T., Veraverbeke, S., Andela, N., Lasslop, G., Forkel, M., Smith, A.J.P., Burton, C., Betts, R.A., van der Werf, G.R., Sitch, S., Canadell, J.G., Santin, C., Kolden, C., Doerr, S.H., Le Quéré, C., 2022. Global and regional trends and drivers of fire under climate change. *Rev. Geophys.* 60, e2020RG000726. <https://doi.org/10.1029/2020RG000726>.
- Katragkou, E., Garcíá-Díez, M., Vautard, R., Sobolowski, S., Zanis, P., Alexandri, G., Cardoso, R.M., Colette, A., Fernandez, J., Gobiet, A., Goergen, K., Karacostas, T., Knist, S., Mayer, S., Soares, P.M.M., Pytharoulis, I., Tegoulia, I., Tsikerdekis, A., Jacob, D., 2015. Regional climate hindcast simulations within EURO-CORDEX: evaluation of a WRF multi-physics ensemble. *Geosci. Model Dev. (GMD)* 8, 603–618. <https://doi.org/10.5194/gmd-8-603-2015>.
- Keeley, J.E., Syphard, A.D., 2021. Large California wildfires: 2020 fires in historical context. *Fire Ecology* 17, 1–11. <https://doi.org/10.1186/s42408-021-00110-7>.
- Knutti, R., Sedláček, J., Sanderson, B.M., Lorenz, R., Fischer, E.M., Eyring, V., 2017. A climate model projection weighting scheme accounting for performance and interdependence. *Geophys. Res. Lett.* 44, 1909–1918. <https://doi.org/10.1002/2016GL072012>.
- Kotlarski, S., Keuler, K., Christensen, O.B., Colette, A., Déqué, M., Gobiet, A., Goergen, K., Jacob, D., Lüthi, D., van Meijgaard, E., Nikulin, G., Schär, C., Teichmann, C., Vautard, R., Warrach-Sagi, K., Wulfmeyer, V., 2014. Regional climate modeling on European scales: a joint standard evaluation of the EURO-
- CORDEX RCM ensemble. *Geosci. Model Dev. (GMD)* 7, 1297–1333. <https://doi.org/10.5194/gmd-7-1297-2014>.
- Lareau, N.P., Clements, C.B., 2017. The mean and turbulent properties of a wildfire convective plume. *J. Appl. Meteorol. Climatol.* 56, 2289–2299. <https://doi.org/10.1175/JAMC-D-16-0384.1>.
- Libonati, R., Pereira, J.M.C., da Camara, C.C., Peres, L.F., Oom, D., Rodrigues, J.A., Santos, F.L.M., Trigo, R.M., Gouveia, C.M.P., Machado-Silva, F., Enrich-Prast, A., Silva, J.M.N., 2021. Twenty-first century droughts have not increasingly exacerbated fire season severity in the Brazilian Amazon. *Sci. Rep.* 11, 1–13. <https://doi.org/10.1038/s41598-021-82158-8>.
- Lima, D.C.A., Lemos, G., Bento, V.A., Nogueira, M., Soares, P.M.M., 2023a. A multi-variable constrained ensemble of regional climate projections under multi-scenarios for Portugal – Part I: an overview of impacts on means and extremes. *Clim Serv* 30, 100351. <https://doi.org/10.1016/j.ciser.2023.100351>.
- Lima, D.C.A., Lemos, G., Nogueira, M., Soares, P.M.M., 2023b. A multi-variable constrained ensemble of regional climate projections under multi-scenarios for Portugal – Part II: sectoral climate indices. *Clim Serv* 30, 100377. <https://doi.org/10.1016/j.ciser.2023.100377>.
- Lorenz, R., Herger, N., Sedláček, J., Eyring, V., Fischer, E.M., Knutti, R., 2018. Prospects and caveats of weighting climate models for summer maximum temperature projections over north America. *J. Geophys. Res. Atmos.* 123, 4509–4526. <https://doi.org/10.1029/2017JD027992>.
- Martin-Vide, J., Lopez-Bustins, J.A., 2006. The western mediterranean oscillation and rainfall in the Iberian peninsula. *Int. J. Climatol.* 26, 1455–1475. <https://doi.org/10.1002/joc.1388>.
- Mills, G.A., McCaw, L., 2010. Atmospheric Stability Environments and Fire Weather in Australia - Extending the Haines Index. CAWCR Technical Report No. 020.
- Moemken, J., Reyers, M., Feldmann, H., Pinto, J.G., 2018. Future changes of wind speed and wind energy potentials in EURO-CORDEX ensemble simulations. *J. Geophys. Res. Atmos.* 123, 6373–6389. <https://doi.org/10.1029/2018JD028473>.
- Molina, M.O., Careto, J.A.M., Gutiérrez, C., Sánchez, E., Soares, P.M.M., 2023. The added value of high-resolution EURO-CORDEX simulations to describe daily wind speed over Europe. *Int. J. Climatol.* 43, 1062–1078. <https://doi.org/10.1002/joc.7877>.
- Molina-Terrén, D.M., Xanthopoulos, G., Diakakis, M., Ribeiro, L., Caballero, D., Delogu, G.M., Viegas, D.X., Silva, C.A., Cardil, A., 2019. Analysis of forest fire fatalities in southern Europe: Spain, Portugal, Greece and sardinia (Italy). *Int. J. Wildland Fire* 28, 85–98. <https://doi.org/10.1071/WF18004>.
- Moriondo, M., Good, P., Duraio, R., Bindi, M., Giannakopoulos, C., Corte-Real, J., 2006. Potential impact of climate change on fire risk in the Mediterranean area. *Clim. Res.* 31, 85–95. <https://doi.org/10.3354/cr031085>.
- Moss, R.H., Edmonds, J.A., Hibbard, K.A., Manning, M.R., Rose, S.K., van Vuuren, D.P., Carter, T.R., Emori, S., Kainuma, M., Kram, T., Meehl, G.A., Mitchell, J.F.B., Nakicenovic, N., Riahi, K., Smith, S.J., Stouffer, R.J., Thomson, A.M., Weyant, J.P., Wilbanks, T.J., 2010. The next generation of scenarios for climate change research and assessment. *Nature*. <https://doi.org/10.1038/nature08823>.
- Nogueira, M., Soares, P.M.M., Tomé, R., Cardoso, R.M., 2019. High-resolution multi-model projections of onshore wind resources over Portugal under a changing climate. *Theor. Appl. Climatol.* 136, 347–362. <https://doi.org/10.1007/s00704-018-2495-4>.
- Nunes, S.A., DaCamara, C.C., Pereira, J.M.C., Trigo, R.M., 2023. Assessing the role played by meteorological conditions on the interannual variability of fire activity in four subregions of Iberia. *Int. J. Wildland Fire*. <https://doi.org/10.1071/WF22137>.
- Oliveira, M., Delerue-Matos, C., Pereira, M.C., Morais, S., 2020. Environmental particulate matter levels during 2017 large forest fires and megafires in the center region of Portugal: a public health concern? *Int. J. Environ. Res. Publ. Health* 17. <https://doi.org/10.3390/ijerph17031032>.
- Parente, J., Pereira, M.G., Amraoui, M., Fischer, E.M., 2018. Heat waves in Portugal: current regime, changes in future climate and impacts on extreme wildfires. *Sci. Total Environ.* 631–632, 534–549. <https://doi.org/10.1016/j.scitotenv.2018.03.044>.
- Pausas, J.G., Fernández-Muñoz, S., 2012. Fire regime changes in the Western Mediterranean Basin: from fuel-limited to drought-driven fire regime. *Clim. Change* 110, 215–226. <https://doi.org/10.1007/s10584-011-0060-6>.
- Peña-Ortiz, C., Barriopedro, D., García-Herrera, R., 2015. Multidecadal variability of the summer length in Europe. *J. Clim.* 28, 5375–5388. <https://doi.org/10.1175/JCLI-D-14-00429.1>.
- Pereira, M.G., Trigo, R.M., da Camara, C.C., Pereira, J.M.C., Leite, S.M., 2005. Synoptic patterns associated with large summer forest fires in Portugal. *Agric. For. Meteorol.* 129, 11–25. <https://doi.org/10.1016/j.agrformet.2004.12.007>.
- Perkins, S.E., Pitman, A.J., Holbrook, N.J., McAneney, J., 2007. Evaluation of the AR4 climate models' simulated daily maximum temperature, minimum temperature, and precipitation over Australia using probability density functions. *J. Clim.* 20, 4356–4376. <https://doi.org/10.1175/JCLI4253.1>.
- Pinto, M.M., Dacama, C.C., Hurdic, A., Trigo, R.M., Trigo, I.F., 2020. Enhancing the fire weather index with atmospheric instability information. *Environ. Res. Lett.* 15, 940–947. <https://doi.org/10.1088/1748-9326/ab9e22>.
- Pinto, M.M., et al., 2018. The extreme weather conditions behind the destructive fires of June and October 2017 in Portugal. In: Advances in Forest Fire Research 2018. Imprensa da Universidade de Coimbra, pp. 138–145. https://doi.org/10.14195/978-989-26-16-506_13.
- Portela, A., Castro, M., 1996. Summer thermal lows in the Iberian peninsula: a three-dimensional simulation. *Q. J. R. Meteorol. Soc.* 122, 1–22. <https://doi.org/10.1002/qj.49712252902>.
- Prein, A.F., Gobiet, A., Truhetz, H., Keuler, K., Goergen, K., Teichmann, C., Fox Maule, C., van Meijgaard, E., Déqué, M., Nikulin, G., Vautard, R., Colette, A., Kjellström, E., Jacob, D., 2016. Precipitation in the EURO-CORDEX 0.11° and 0.44°

- simulations: high resolution, high benefits? *Clim. Dynam.* 46, 383–412. <https://doi.org/10.1007/s00382-015-2589-y>.
- Ramos, A.M., Russo, A., DaCamara, C.C., Nunes, S., Sousa, P., Soares, P.M.M., Lima, M.M., Hurduc, A., Trigo, R.M., 2023. The Compound Event that Triggered the Destructive Fires of October 2017 in Portugal. *iScience*, 106141. <https://doi.org/10.1016/j.isci.2023.106141>.
- Riahi, K., Rao, S., Krey, V., Cho, C., Chirkov, V., Fischer, G., Kindermann, G., Nakicenovic, N., Rafaj, P., 2011. RCP 8.5-A scenario of comparatively high greenhouse gas emissions. *Clim. Change* 109, 33–57. <https://doi.org/10.1007/s10584-011-0149-y>.
- Rockel, B., Will, A., Hense, A., 2008. The regional climate model COSMO-CLM (CCLM). *Meteorol. Zeitschrift*. <https://doi.org/10.1127/0941-2948/2008/0309>.
- Rodrigues, M., Jiménez-Ruano, A., de la Riva, J., 2019. Fire regime dynamics in mainland Spain. Part 1: drivers of change. *Sci. Total Environ.* 721, 135841 <https://doi.org/10.1016/j.scitotenv.2019.135841>.
- Ruffault, J., Curt, T., Martin-Stpaul, N.K., Moron, V., Trigo, R.M., 2018. Extreme wildfire events are linked to global-change-type droughts in the northern Mediterranean. *Nat. Hazards Earth Syst. Sci.* 18, 847–856. <https://doi.org/10.5194/nhess-18-847-2018>.
- Rummukainen, M., 2016. Added value in regional climate modeling. *Wiley Interdiscip. Rev. Clim. Chang.* 7, 145–159. <https://doi.org/10.1002/wcc.378>.
- Russo, A., Gouveia, C.M., Páscoa, P., DaCamara, C.C., Sousa, P.M., Trigo, R.M., 2017. Assessing the role of drought events on wildfires in the Iberian Peninsula. *Agric. For. Meteorol.* 237–238, 50–59. <https://doi.org/10.1016/j.agrformet.2017.01.021>.
- Salis, M., Ager, A.A., Arcà, B., Finney, M.A., Bacciu, V., Duce, P., Spano, D., 2013. Assessing exposure of human and ecological values to wildfire in Sardinia, Italy. *Int. J. Wildland Fire* 22, 549–565. <https://doi.org/10.1071/WF11060>.
- Sánchez-Benítez, A., García-Herrera, R., Barriopedro, D., Sousa, P.M., Trigo, R.M., 2018. 2017: the earliest European summer mega-heatwave of reanalysis period. *Geophys. Res. Lett.* 45, 1955–1962. <https://doi.org/10.1002/2018GL077253>.
- Sanderson, B.M., Wehner, M., Knutti, R., 2017. Skill and independence weighting for multi-model assessments. *Geosci. Model Dev. (GMD)* 10, 2379–2395. <https://doi.org/10.5194/gmd-10-2379-2017>.
- Santos, L.C., Lima, M.M., Bento, V.A., Nunes, S.A., DaCamara, C.C., Russo, A., Soares, P.M.M., Trigo, R.M., 2023. An evaluation of the atmospheric instability effect on wildfire danger using ERA5 over the Iberian peninsula. *Fire* 6, 120. <https://doi.org/10.3390/fire6030120>.
- San-Miguel-Ayanz, J., Schulte, E., Schmuck, G., Camia, A., Strobl, P., Liberta, G., Giovando, C., Boca, R., Sedano, F., Kempeneers, P., McInerney, D., Withmore, C., de Oliveira, S.S., Rodrigues, M., Durrant, T., Corti, P., Oehler, F., Vilar, L., Amatulli, G., 2012. Comprehensive monitoring of wildfires in Europe: the European forest fire information system (EFFIS). In: *Approaches to Managing Disaster - Assessing Hazards, Emergencies and Disaster Impacts*. IntechOpen. <https://doi.org/10.5772/28441>.
- Soares, P.M.M., Cardoso, R.M., 2018. A simple method to assess the added value using high-resolution climate distributions: Application to the EURO-CORDEX daily precipitation. *Int. J. Climatol.* 38, 1484–1498. <https://doi.org/10.1002/joc.5261>.
- Soares, P.M.M., Cardoso, R.M., Lima, D.C.A., Miranda, P.M.A., 2017a. Future precipitation in Portugal: high-resolution projections using WRF model and EURO-CORDEX multi-model ensembles. *Clim. Dynam.* 49, 2503–2530. <https://doi.org/10.1007/s00382-016-3455-2>.
- Soares, P.M.M., Cardoso, R.M., Miranda, P.M.A., de Medeiros, J., Belo-Pereira, M., Espírito-Santo, F., 2012. WRF high resolution dynamical downscaling of ERA-Interim for Portugal. *Clim. Dynam.* 39, 2497–2522. <https://doi.org/10.1007/s00382-012-1315-2>.
- Soares, P.M.M., Lima, D.C.A., Cardoso, R.M., Nascimento, M.L., Semedo, A., 2017b. Western Iberian offshore wind resources: more or less in a global warming climate? *Appl. Energy* 203, 72–90. <https://doi.org/10.1016/j.apenergy.2017.06.004>.
- Soares, P.M.M., Lima, D.C.A., Cardoso, R.M., Semedo, A., 2017c. High resolution projections for the western Iberian coastal low level jet in a changing climate. *Clim. Dynam.* 49, 1547–1566. <https://doi.org/10.1007/s00382-016-3397-8>.
- Sousa, P.M., Trigo, R.M., Pereira, M.G., Bedia, J., Gutiérrez, J.M., 2015. Different approaches to model future burnt area in the Iberian Peninsula. *Agric. For. Meteorol.* 202, 11–25. <https://doi.org/10.1016/j.agrformet.2014.11.018>.
- Stocks, B.J., Lynham, T.J., Lawson, B.D., Alexander, M.E., Wagner, C.E. van, McAlpine, R.S., Dubé, D.E., 1989. The Canadian forest fire danger rating system: an overview. *For. Chron.* 65, 450–457. <https://doi.org/10.5558/tfc65450-6>.
- Strandberg, G., Bärring, L., Hansson, U., Jansson, C., Jones, C., Kjellström, E., Kolax, Michael, Marco Kupiainen, G., Nikulin, P.S., Wang, A.U., 2014. CORDEX scenarios for Europe from the Rossby Centre regional climate model RCA4. *Rep. Meteorol. Clim.* 116, 1–84.
- Trigo, I.F., Bigg, G.R., Davies, T.D., 2002. Climatology of cyclogenesis mechanisms in the Mediterranean. *Mon. Weather Rev.* 130, 549–569. [https://doi.org/10.1175/1520-0493\(2002\)130<0549:COCMIT>2.0.CO](https://doi.org/10.1175/1520-0493(2002)130<0549:COCMIT>2.0.CO).
- Trigo, I.F., Dacama, C.C., Viterbo, P., Roujean, J.-L., Olesen, F., Barroso, C., Camacho-de-Coca, F., Carrer, D., Freitas, S.C., García-Haro, J., Geiger, B., Gellens-Meulenberghs, F., Ghilain, N., Meliá, J., Pessanha, L., Siljamo, N., Arboleda, A., 2011. The satellite application facility for land surface analysis. *Int. J. Rem. Sens.* 32, 2725–2744. <https://doi.org/10.1080/0143161003743199>.
- Trigo, R.M., Pereira, J.M.C., Pereira, M.G., Mota, B., Calado, T.J., Dacama, C.C., Santo, F.E., 2006. Atmospheric conditions associated with the exceptional fire season of 2003 in Portugal. *Int. J. Climatol.* 26, 1741–1757. <https://doi.org/10.1002/joc.1333>.
- Trigo, R.M., Sousa, P.M., Pereira, M.G., Rasilla, D., Gouveia, C.M., 2016. Modelling wildfire activity in Iberia with different atmospheric circulation weather types. *Int. J. Climatol.* 36, 2761–2778. <https://doi.org/10.1002/joc.3749>.
- Trnka, M., Možný, M., Jurečka, F., Balek, J., Semerádová, D., Hlavinka, P., Štěpánek, P., Farda, A., Skalák, P., Cienciala, E., Čermák, P., Chuchma, F., Zahradníček, P., Janouš, D., Fischer, M., Žalud, Z., Brázdił, R., 2021. Observed and estimated consequences of climate change for the fire weather regime in the moist-temperate climate of the Czech Republic. *Agric. For. Meteorol.* 310, 108583 <https://doi.org/10.1016/j.agrformet.2021.108583>.
- Turco, M., Jerez, S., Augusto, S., Tarín-Carrasco, P., Ratola, N., Jiménez-Guerrero, P., Trigo, R.M., 2019. Climate drivers of the 2017 devastating fires in Portugal. *Sci. Rep.* 9, 1–8. <https://doi.org/10.1038/s41598-019-50281-2>.
- Turco, M., Rosa-Cánovas, J.J., Bedía, J., Jerez, S., Montávez, J.P., Llasat, M.C., Provenzale, A., 2018. Exacerbated fires in Mediterranean Europe due to anthropogenic warming projected with non-stationary climate-fire models. *Nat. Commun.* 9, 1–9. <https://doi.org/10.1038/s41467-018-06358-z>.
- van Meijgaard, E., van Ulft, L.H., van de Berg, W.J., Bosveld, F.C., den Hurk, B.J.M., Lenderink, G., Siebesma, A.P., 2008. The KNMI regional atmospheric model RACMO version 2.1. *Technical Report 302*.
- van Vuuren, D.P., Edmonds, J., Kainuma, M., Riahi, K., Thomson, A., Hibbard, K., Hurtt, G.C., Kram, T., Krey, V., Lamarque, J.F., Masui, T., Meinshausen, M., Nakicenovic, N., Smith, S.J., Rose, S.K., 2011. The representative concentration pathways: an overview. *Clim. Change* 109, 5–31. <https://doi.org/10.1007/s10584-011-0148-z>.
- van Wagner, C.E., 1987. Development and Structure of the Canadian Forest Fire Weather Index System.
- van Wagner, C.E., 1974. A spread index for crown fires in spring. *Inf. Rep.* 55, 9.
- Varela, V., Vlachogiannis, D., Sfetsos, A., Karozis, S., Politis, N., Giroud, F., 2019. Projection of forest fire danger due to climate change in the French Mediterranean region. *Sustainability* 11, 4284. <https://doi.org/10.3390/su11164284>.
- Vautard, R., Gobiet, A., Jacob, D., Belda, M., Colette, A., Déqué, M., Fernández, J., García-Díez, M., Goergen, K., Gütterl, I., Halenka, T., Karacostas, T., Katragkou, E., Keuler, K., Kotlarski, S., Mayer, S., van Meijgaard, E., Nikulin, G., Patarčić, M., Scinocca, J., Sobolowski, S., Suklitsch, M., Teichmann, C., Warrach-Sagi, K., Wulfmeyer, V., Yiou, P., 2013. The simulation of European heat waves from an ensemble of regional climate models within the EURO-CORDEX project. *Clim. Dynam.* 41, 2555–2575. <https://doi.org/10.1007/s00382-013-1714-z>.
- Wenzel, S., Eyring, V., Gerber, E.P., Karpechko, A.Y., 2016. Constraining future summer austral jet stream positions in the CMIP5 ensemble by process-oriented multiple diagnostic regression. *J. Clim.* 29, 673–687. <https://doi.org/10.1175/JCLI-D-15-0412.1>.
- Zhang, X., Hegerl, G., Zwiers, F.W., Kenyon, J., 2005. Avoiding inhomogeneity in percentile-based indices of temperature extremes. *J. Clim.* 18, 1641–1651. <https://doi.org/10.1175/JCLI3366.1>.